AD-A094 828 ARMY ELECTRONICS RESEARCH AND DEVELOPMENT COMMAND WS--ETC F/G 4/2
EVALUATION OF THE ENVIRONMENTAL INSTRUMENTS, INCORPORATED SERIE--ETC(U)
SEP 80 W J VECHIONE

UNCLASSIFIED ERADCOM/ASL-TR-0067

NL

1 OF 1
AD A094828

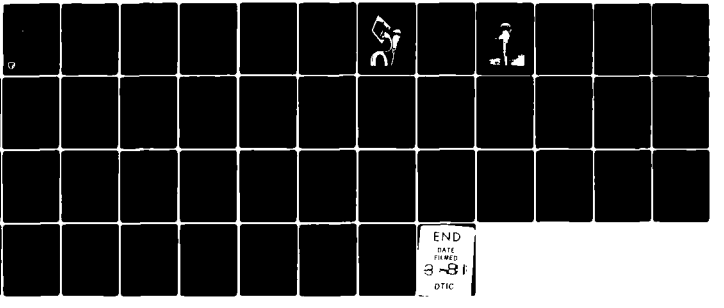

END
DATE FILMED
3-81
DTIC

LEVEL II

12

ERADCOM/ASL-TR-0067

AD

Reports Control Symbol
OSD 1366

EVALUATION OF THE ENVIRONMENTAL INSTRUMENTS, INCORPORATED SERIES 200 DUAL COMPONENT WIND SET.

SEPTEMBER 1980

By

W.J. VECHIONE

Approved for public release; distribution unlimited

US Army Electronics Research and Development Command
ATMOSPHERIC SCIENCES LABORATORY
White Sands Missile Range, NM 88002

NOTICES

Disclaimers

The findings in this report are not to be construed as an official Department of the Army position, unless so designated by other authorized documents.

The citation of trade names and names of manufacturers in this report is not to be construed as official Government indorsement or approval of commercial products or services referenced herein.

Disposition

Destroy this report when it is no longer needed. Do not return it to the originator.

SECURITY CLASSIFICATION OF THIS PAGE *(When Data Entered)*

REPORT DOCUMENTATION PAGE		READ INSTRUCTIONS BEFORE COMPLETING FORM
1. REPORT NUMBER ASL-TR-0067	2. GOVT ACCESSION NO. AD-A094 828	3. RECIPIENT'S CATALOG NUMBER
4. TITLE *(and Subtitle)* EVALUATION OF THE ENVIRONMENTAL INSTRUMENTS, INCORPORATED SERIES 200 DUAL COMPONENT WIND SET		5. TYPE OF REPORT & PERIOD COVERED R&D Technical Report 6. PERFORMING ORG. REPORT NUMBER
7. AUTHOR(s) W. J. Vechione		8. CONTRACT OR GRANT NUMBER(s)
9. PERFORMING ORGANIZATION NAME AND ADDRESS Atmospheric Sciences Laboratory White Sands Missile Range, NM 88002		10. PROGRAM ELEMENT, PROJECT, TASK AREA & WORK UNIT NUMBERS DA Task No. 1F263741D158
11. CONTROLLING OFFICE NAME AND ADDRESS US Army Electronics Research and Development Command Adelphi, MD 20783		12. REPORT DATE September 1980 13. NUMBER OF PAGES 39
14. MONITORING AGENCY NAME & ADDRESS*(if different from Controlling Office)*		15. SECURITY CLASS. *(of this report)* UNCLASSIFIED 15a. DECLASSIFICATION/DOWNGRADING SCHEDULE

16. DISTRIBUTION STATEMENT *(of this Report)*

Approved for public release; distribution unlimited.

17. DISTRIBUTION STATEMENT *(of the abstract entered in Block 20, if different from Report)*

18. SUPPLEMENTARY NOTES

19. KEY WORDS *(Continue on reverse side if necessary and identify by block number)*

Hot wire anemometer
Crosswinds
Pressure
Temperature

20. ABSTRACT *(Continue on reverse side if necessary and identify by block number)*

Tests of atmospheric parameter measurements using the EII Series 200 Dual Component Wind Set with integral pressure and temperature sensors were made during the period of May 1977 through March 1978. These tests included laboratory comparison, wind tunnel, and field operation tests. Data collected with the sensor were compared to calibrated standards. Presented in this report are all tabulated and graphic representation as well as field operation results. The results of the test show the systems relative comparison with

DD FORM 1 JAN 73 1473 EDITION OF 1 NOV 65 IS OBSOLETE

SECURITY CLASSIFICATION OF THIS PAGE *(When Data Entered)*

20. ABSTRACT (cont)

the calibrated standards of temperature and pressure. Wind measurements became more comparable with increasing windspeeds. A method of utilizing the entire windspeed capability range of the sensor is proposed.

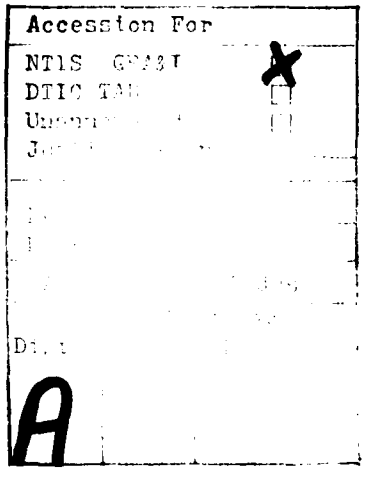

CONTENTS

1. INTRODUCTION

The state of the atmosphere in an area of tactical operations affects Army operations within that area. When commanders and their staff cannot obtain current localized weather information from remote areas of the zone of operations, they are limited in acquiring vital information necessary for operational planning and execution. A system of unmanned portable automatic weather stations is required to satisfy the need to supply the information for day-to-day tactical operations and long-range operations planning.

A system was designed as an experimental prototype and subsequently qualified for advanced development planning by the Atmospheric Sciences Laboratory (ASL). This system measured windspeed, wind direction, atmospheric pressure, temperature, and relative humidity. However, the wind sensors used in the experimental prototype were modified standards, with mechanically active (moving) wind sensor elements, and one tactical requirement demanded that the sensor elements be mechanically passive.

After evaluation of different types of sensors that could potentially apply for this application, the EII Series 200 Dual Component Wind Set with integral pressure and temperature sensing was chosen for applications testing. One set was procured for evaluation as a possible sensor package for the advanced development system.

The series 200 wind component system (figure 1) is a hot wire anemometer device with the sensor head containing the various sensor components packaged in a wire-shielded enclosure and the various linearization and control circuitry housed in a separate enclosure. Power requirement is 28 V dc.

Results of collected data are presented in this report, with an evaluation and analysis that determine the accuracy, reliability, and applicability of the series 200 sensor.

The system was subjected to controlled environmental testing at the White Sands Missile Range (WSMR) calibration laboratory facility for pressure and temperature tests, and at the ASL wind tunnel facility for wind measurement tests. Also, during February to April 1978, the instrument was tested at Biggs Optical Range (BOR), Fort Bliss, Texas, in a field environment.

2. TEST OBJECTIVES

Several remote meteorological sensor systems have been developed and placed into operation within the last 10 years. A number of these systems were evaluated for tactical army use, but none possessed all the necessary characteristics. Recurring noncompliance was found in the sensor subsystems in particular. The user representative of the tactical army indicated that a mechanically passive sensor system was required, and the most promising sensor type satisfying this requirement was the hot wire or hot film anemometer type sensors. The system tested and reported on herein was determined to best meet the criteria of sensor requirements.

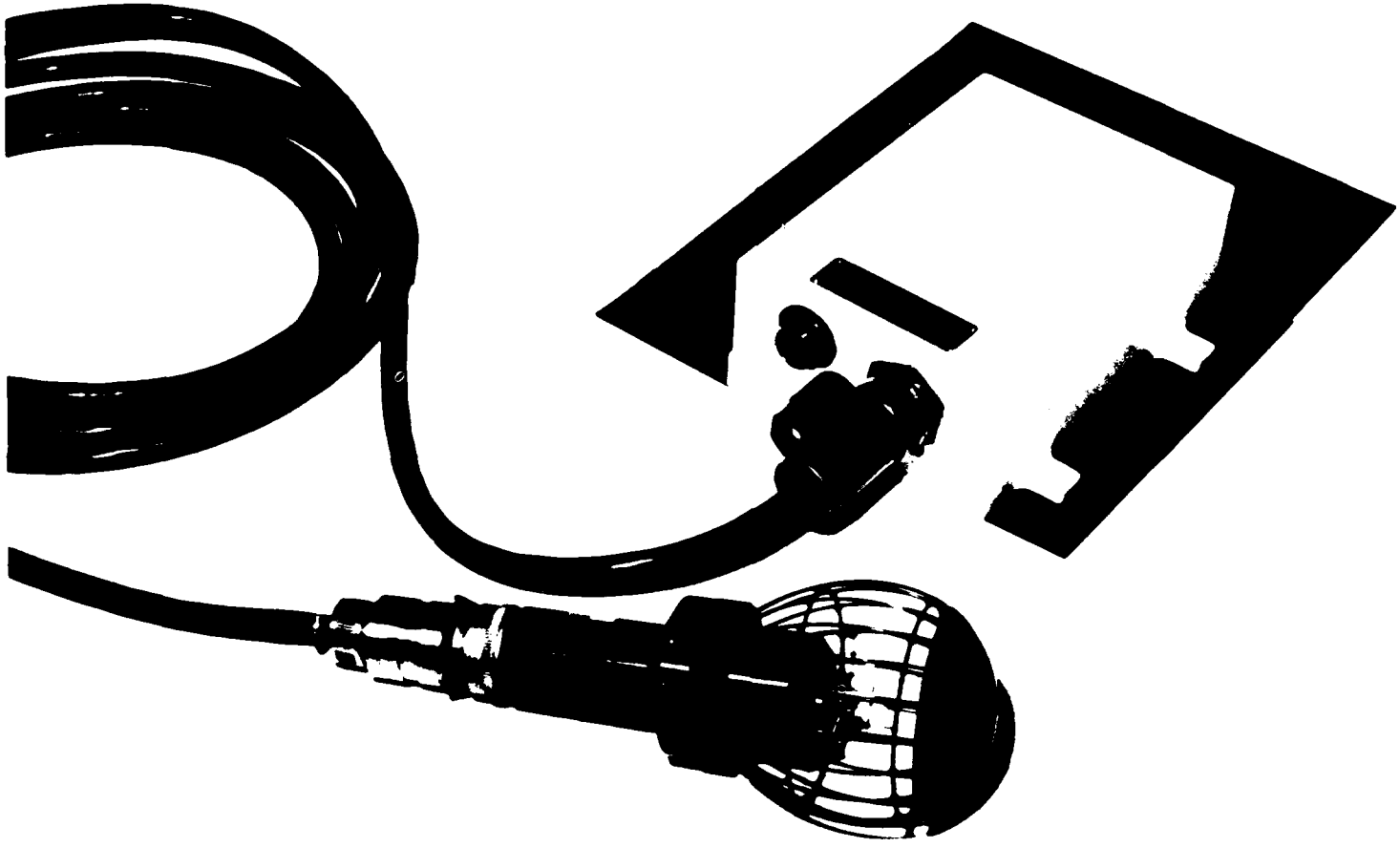

Figure 1. Probe head with electronics enclosure.

The objectives of the series of tests performed on the series 200 wind set were:

a. Determine the actual capability of the sensor system in accuracy of measurements.

b. By operating the system in a field environment, determine the ease or difficulty of operation setup and use, and compare operation with research grade colocated systems.

c. Contribute to the data base for continued remote meteorological sensor development to satisfy stated requirements.

3. SYSTEM DESCRIPTION AND OPERATIONAL THEORY

3.1 Sensors

The EII Series 200 Dual Component Wind Set (figures 1 and 2) provides the measurement of two 90-degree components of windspeed, ambient pressure, and barometric pressure. The wind components are measured by two pairs of heated resistive sensing elements, placed at right angles to each other in the horizontal plane. The outputs of these elements are processed in a manner that yields sine and cosine functions of the wind vector blowing against the sensing elements.

Ambient temperature is measured by a platinum resistance temperature sensor which exhibits a resistance of approximately 200 ohms at $0^{o}C$ and is calibrated over a range of $-70^{o}C$ to $+40^{o}C$.

Atmospheric pressure is measured with a 0 to 15 psia pressure transducer capped by a four-port cap to provide stagnant air at the transducer input port. The electronics linearize the output between 9.8 and 15.7 psia (corresponding to 20 to 32 inches of mercury).

3.2 Probe Operation[1]

Each wind component is measured by a film resistance sensor constructed of two closely spaced wire elements. These elements are supported in a manner which provides thermal isolation between the elements so as to determine instantaneous windspeed and wind direction. The pair is continuously joined along their length, and one element serves as a leading wire. Flow between the elements is prevented by the bridging material. Their cross-sectional area (1.4 mm) is much smaller than their length (31 mm). Each element consists of a ceramic substrate supporting a metallic film which is in turn protected by a glazed fused silica coating. The metallic film is stable and has a high positive temperature coefficient of resistance. Wires are attached to both ends of the elements which then form two series resistances in one arm of a

[1]Description and theory of operation for the dual axis, pressure and temperature instrument, Series 200, Model 255, Environmental Instruments, Incorporated, 4 Mercer Road, Natick, MA 07760

Figure 5. Probe head in test configuration (field test).

Wheatstone bridge. The wires are electrically excited so that total resistance is constantly maintained by a closed loop feedback amplifier. The potential at the junction of the two series connected resistive elements is sensed to derive the sign (+ or -), which indicates the wind direction across the element pair. The reference arm of the Wheatstone bridge incorporates a temperature sensor whose temperature coefficient is adjusted to compensate the wind sensing element pair which is best described as a heat loss mass flow sensor and is operated at a constant temperature elevation above sensed ambient temperature.

The total voltage appearing across the sensing element pair is used to indicate P_v, mass flow. The windspeed output signal is nonlinear and contains a constant zero velocity self-heating signal, a fourth root term as a function of airflow velocity and turbulence components which result from gustiness in the airflow. The signal conditioning electronics within the probe are used to zero the output for zero wind conditions and set the full-scale output signal for each axis.

A comparator is connected across the sensing element pair to detect the electrical change of the sensing element midpoint as the wind shifts in direction on either side of the sensing element air. The comparator output is connected to an external pack which contains linearization circuitry and a polarity output amplifier whose output sign switches positive or negative as the wind shifts direction.

In general the final output is in the form of

$$\frac{P_a}{P_r} = V_w \text{ Cosine } \alpha \text{ for the crosswind axis,}$$

and

$$\frac{P_a}{P_r} = V_w \text{ Sine } \alpha \text{ for the headwind axis,}$$

where P_a is the ambient air density, P_r is reference density at standard conditions, V_w is the windspeed, and α is the azimuth angle of the wind vector. A discussion of this wind direction determination follows.

3.2.1 Determination of Wind Direction

The probe is constructed with two paired coplanar axial elements sensor wires. Within each sensor pair, one wire element is biased positively and one negatively. The wires exposed to horizontal windflow will exhibit a positive output when the positively based wire is "upstream" and allow a negative output when the negatively biased wire elements is upstream. The theory requires the elements to be maintained at a steady heat state. Therefore, in the presence of wind, cooling by its passage, the elements require greater current and voltage to the upstream wire. This voltage rise is proportional to the output. Since the probe is fixed, any wind other than from 90 degrees (i.e., directly perpendicular to the wire pair) will result in a vector of wind impinging the sensor pair. Thus, using only one pair, the angle of wind

vector will result in two force components W_v Cos θ and W_v Sin θ. However, the force component values from θ in the first quadrant or second quadrant are equivalent, i.e.,

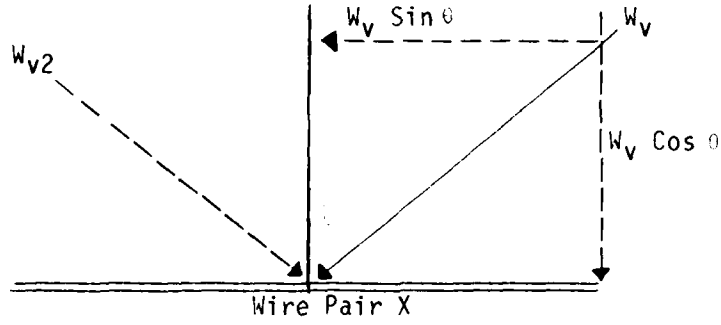

Winds W_v and W_{v2} yield equal output from wire pair X
(i.e., no direction is discernible)

The value of concern is W_v Cos θ, because W_v Sin θ is parallel to the wire elements and impinges only the diametric cross section of the wire pair, not the main perpendicular area. Therefore, the wind velocity of interest to this pair of wire elements is essentially equal to W_v Cos θ. By positioning a second set of wire elements perpendicular to the original pair, biased in the same manner, the actual direction can be derived. Plus bias is on the right element of the vertical pair and the top elements of the horizontal pair as shown below:

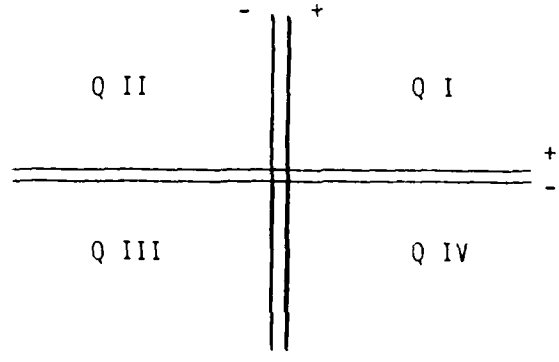

Therefore, for finding directivity, a wind from quadrant I will result in a positive output from both elements. In contrast, a wind from quadrant III will result in negative outputs from both elements.

3.2.2 Pressure

The pressure transducer is a hybrid linear silicon device which consists of a diaphragm and pressure reference, piezoresistive sensor, signal discriminator, voltage reference, and amplifier. It is physically small, and the port is located under a vented structure mounted below the two wind sensing elements. The range of interest for the meteorological sensor is from 20.00 inches (9.824 psi) to 32.00 inches (15.7184 psi) of mercury.

3.2.3 Temperature

The ambient temperature transducer is a platinum resistance spiral contained within an aluminum oxide shell. It is mounted on two posts alongside the pressure port. The temperature transducer is a device whose resistance is characterized as a function of temperature. Temperature and pressure signal conditioning amplifiers are contained within the probe and a third amplifier is used to provide temperature compensation of the pressure output by the temperature output signal. These conditioning amplifiers provide scaling and offset corrections for both the temperature and pressure output signals to the external electronics pack.

3.2.4 Electronics Pack

The power supply section, wind sensor excitation circuits, and wind output signal processing circuits are contained within a sealed aluminum housing.

3.2.4.1 Power Section. DC power input is regulated to +19 V for the wind axis bridge derive potential and +10 V switching regulator. Reverse voltage and overvoltage protection are inherent in the design. Inversion of the +10 V to a comparator circuit yields -17.8 V output, which, along with the +19 V, supplies a dual tracking voltage regulator for a +15 V supply to the operational amplifiers of the subsystem. Tolerance of wide input voltage swings is integral, and at the low end integrity of the -15 V output line is maintained.

3.2.4.2 Wind Card. Both axes, headwind and crosswind, use similar wind cards. The headwind cards are interchangeable, and the crosswind cards differ only in the resistance component values used in function generator circuit for linearization of the probe signals.

The nonlinear probe signal for each axis is applied to a function generator circuit whose gain transfer characteristic is inverse to the probe signal transfer function. The circuit is temperature compensated so that the resulting function generator output is temperature stabilized. The linearizer output is unipolar, 0 to 10 V full-scale, for all directions of wind input. The linearized wind signal feeds a switchable gain amplifier controlled by a comparator which is connected and follows the sign sense signals. The signs sense amplifier operates as a unity gain follower amplifier in one case and as an inverting amplifier in a wind reversal case. The gain is trimmed by a "lobe trim" resistor. Each lobe of the wind sensor has equivalent overall sensitivity. The sensing elements, being nonideal due to manufacturing, etc., do not follow a cosine law over all angles to ±90 degrees from normal flow. To correct for this, a "dither" signal is generated at 400 Hz and injected into the comparator circuit with the sign sense signal to facilitate switching from lobe to lobe at low wind angles.

The effect of the dither signal near the wind signal axis crossings is a smoother transition through the zero value region of the output waveform.

The output of the switchable gain amplifier is fed to an inverting amplifier which has filter characteristics with a nominal frequency cutoff value of 1 Hz.

The gain of the output stage is set at about 0.5 with ±5 V corresponding to ±25 m/s windspeed. Final output is limited by a zener diode to about ±10 V for overrange wind conditions.

The bridge driver is a differential amplifier followed by an emitter follower current booster amplifier feeding the top of the probe Wheatstone bridge. The differential amplifier inputs are connected to the bridge error points through 10 K ohm resistors used to isolate cable capacitance.

If the amplifier is close to balance, for the input voltage and currents, the bridge driver cannot turn on when power is first supplied, as no potential is applied to the bridge. To overcome this feature a series voltage divider is gated to the amplifier reference input to provide an initial offset voltage which causes a small bridge current to flow. All these circuits are contained within a closed loop negative feedback system.

Initially, the bridge is unbalanced. Only when current flows through the sensing elements will the resistance value increase so as to cause and maintain bridge balance. It is this characteristic which allows the determination of the power which must be automatically added to the sensing elements to equal the power lost by wind induced cooling.

4. TEST SUPPORT

4.1 Meteorological Optical Measurement System

The meteorological optical measurement system (MOMS) is a mobile, self-contained data collection and reduction system containing analog and digital subsystems specifically engineered for the measurement and recording of atmospheric meteorological data. The system uses an HP 2100 computer system as a controller and is managed by an in-house developed program that samples the various sensors at preset rates, stores the data, and then reduces and analyzes the data according to the program requirements. Output format capabilities are raw scatter graphs, time averaged plots, printer, limited strip chart, and digital tape. During these tests, analog wind data from the co-located anemometer and the series 200 sensor output were recorded on digital tape. Other meteorological data simultaneously recorded were atmospheric pressure, temperature, refractive index structure coefficient, and dew point. Plotting of the data plots of the series 200 versus the "baseline" anemometer was accomplished off-line.

4.2 WSMR Calibration Laboratory and Wind Tunnel Facility

Pressure and temperature laboratory comparison testing was done at the WSMR calibration laboratory. The series 200 sensor was tested against National Bureau of Standards (NBS) traceable baseline instrumentation.

Temperature measurements were made in a Tenny "TH-Jr" Model 76H502 temperature/humidity chamber with a calibrated readout using a platinum resistance thermometer sensor. Testing commenced after a 4-hour stabilization cycle and was cycled low-high-low.

Pressure tests were made in a pressure chamber using a Quartz Bourdon pressure readout calibrated with a dead weight piston gauge. A three-run average test was performed, cycling low-high-low.

Wind tunnel testing was done at the ASL wind tunnel facility, which is a closed loop tunnel with a 4- by 4- by 6-foot test area. Velocity capability of the tunnel is 85 mi/h and is measured by two sensors: below 10 mi/h by a Pitot-tube-eddy shedding hot wire anemometer, and above 10 mi/h by a manometer.

5. TEST DESCRIPTION

5.1 Laboratory

The pressure and temperature tests were performed by using standard test procedures of the WSMR calibration laboratory. Temperature measurements were made after the test item and chamber stabilized. Pressure measurements were taken 1 min after a pressure step change was introduced. Wind measurements were accomplished in the following manner: (1) the sensor was mounted on a rotating table within the test area and connected to the control electronics and readout outside the tunnel test area, (2) the wind velocity was stabilized at one of five tested velocities, and (3) measurements were made as the test instrument was rotated in 15-degree increments through 360 degrees. The measured headwind and crosswind, the "true" computed headwind and crosswind, and the error differential between these values were computed, and the polar magnitude and phase were plotted.

5.2 Setup for Field Comparisons

Actual field measurement conditions using calibrated baseline instruments were made on the series 200 instrument in conjunction with a multisensor test period during February and March 1978 at the ASL BOR, Fort Bliss, Texas. Data were taken from a colocated RM Young UVW anemometer coaligned with the series 200 sensor. The W or vertical component value was not used in these tests, only the measure U (headwind) and V (crosswind). Data were measured and recorded, and results were displayed by using the MOMS data collection van (see paragraph 4.1).

6. DATA COLLECTION AND RESULTS

6.1 Field Test Data

The operations program of the MOMS computer is designed for acceptance and comparison of data from an unknown sensor versus a known anemometer array. This array consists of up to 40 crosspath anemometers in a 2 km path length. Therefore, in comparing one known anemometer against the test series 200 anemometer, the reduction program was not used. However, the data collection

capability was used for subsequent off-line reduction. Standard deviations of samples and population were calculated by using:

$$S = \sqrt{\frac{\sum_{i=1}^{n} x_i^2 - n\bar{x}^2}{n - 1}} \qquad \text{(Samples)}$$

$$\sigma = \sqrt{\frac{\sum_{i=1}^{n} x_i^2 - n\bar{x}^2}{n}} \qquad \text{(Population)}$$

For 3-min averages

6.2 Laboratory/Wind Tunnel Data

The data collected in the calibration laboratory and wind tunnel tests are the best indicator of the operation of the system since all true values of measured parameters were controlled. The data observed are as follows.

6.2.1 Pressure

Measured over the range of 18.59 to 32.20 inches of mercury. Calculated output voltage was based on

$$V_{out} = \frac{\text{Pressure (inHg)} - 29.93}{2.268}$$

where

29.93 = pressure

V_{out} = zero

2.268 = instrument constant $\frac{P_{max} - P_{min}}{V_{total}} = \frac{32.2 - 18.59}{6}$

6.2.2 Temperature

The temperature data were collected over a test cycle of -45°C to +75°C (true measurement). The output in volts was recorded and the formula: $(V_t \times 11.0) + 15$ was used to compute the instrument-sensed temperature, where V_t = voltage output and 11 = instrument constant derived from: $\frac{Tmax - Tmin}{V_{out\ max}} = \frac{70 - (-40)}{10}$

6.2.3 Winds

Data were recorded by rotating the instrument in 15-degree increments into the mean windflow (held constant per test). Data recorded were: true crosswind (based on a 1 V = 5 m/s sinusoid response), true headwind (based on a 1 V = 5 m/s sinusoid response), measured headwinds and crosswinds, headwind and crosswind errors from true, and polar magnitude and polar phase and their respective errors (this is an indication of true sensor error in wind magnitude and direction).

Headwind and crosswind errors were derived by:

$$\frac{\text{measured value - "true" value}}{\text{"true" value}} \times 100 = \% \text{ error} .$$

Polar coordinates were derived by using a measured crosswind value as ordinate and measured headwind value as abscissa for deriving vector magnitude (P_v) and wind angle (0).

6.3 Results of Data Analysis

Results of the tests are shown in the data figures of appendix A. The deviation magnitude of measured from expected values varied primarily according to the actual windspeed.

In appendix A, the data are presented in the following order: wind tunnel windspeed tests at five velocities, pressure in three runs, temperature, and field wind measurement comparison tests.

During field tests, low windspeeds prevailed. Climatologic data of the region generally indicate that during the time of year that the tests were made, low windspeeds are to be expected. The tests were made at this time to satisfy equipment availability, not expected wind conditions.

Appendix B shows daily weather parameters during the data periods.

6.3.1 Windspeed Tests

The windspeed tests performed in the wind tunnel facility are shown in figures A-1 through A-10, representing data taken at five wind velocities. Data plotted are the true crosswinds and headwinds (i.e., computed expected values), measured crosswinds and headwinds, and errors between true and measured for each 15 degrees of sensor rotation.

The results shown are summarized as follows:

a. Figures A-1 and A-2. At 5 m/s, maximum error in crosswind is 63 percent at 60 and 120 degrees rotation, and real value differences are 0.58 V. Headwind maximum error is 33 percent at 0 degrees with 0.36 V real value difference. Phase error maximum is 15 percent at 60 degrees.

b. Figures A-3 and A-4. At 8.5 m/s, maximum error in crosswinds is 78 percent at 30 and 120 degrees rotation, with real value differences of 0.67 V. Headwind maximum error is 40 percent at 225 degrees, with a real value difference of 0.49 V. Maximum phase error occurs at 165 degrees.

c. Figures A-5 and A-6. At 13 m/s, maximum crosswind error is 53 percent at 165 degrees rotation, with a real value difference of 0.36 V. Headwind maximum error is 35 percent at 300 degrees, with a real value difference of 0.47 V. Maximum phase error is 14 percent at 30 degrees rotation.

d. Figures A-7 and A-8. At 18 m/s, maximum crosswind error is 66 percent at 165 degrees rotation, with a real value difference of 0.59 V. Maximum headwind error is 23 percent at 180 degrees with a real value difference of 0.8 V. Maximum phase error is -15 percent at 165 degrees rotation.

e. Figures A-9 and A-10. At 22 m/s, maximum crosswind error is 68 percent at 165 degrees rotation, with a real value difference of 0.77 V. Headwind maximum error is 26 percent at 195 degrees rotation, with a real value difference of 1.0 V. Maximum phase error of 15 percent occurs at 165 degrees rotation.

Table 1 is a synopsis of wind error.

TABLE 1. WIND ERRORS

Speed (m/s)	Max Crosswind Error (%/V)	Angle of Attack (deg)	Max Headwind Error (%/V)	Angle of Attack (deg)	Max Phase Error (%)	Angle of Attack (deg)
5	63/0.58	60/120	33/0.36	0	15	60
8.5	78/0.67	30/120	40/0.49	225	24	165
13	53/0.36	165	35/0.47	300	14	30
18	66/0.59	165	23/0.8	180	15	165
22	68/0.77	165	26/1.0	195	15	165

6.3.2 Pressure Tests

The pressure tests results are shown in figures A-11 through A-14 and indicate three runs cycled low-high, high-low, and low-high, respectively. Linearity of the output voltage proportional to pressure is excellent, and hysteresis is

minimal. However, a bias voltage of about 0.18 V is evident from the expected output. This bias can be corrected by internal circuit amplifier trim adjustment (and has been accomplished since the tests were made). A major problem with the use of this sensor for atmospheric sensing is its wide range of sensing. Because in situ atmospheric pressure changes occur in a small segment of the overall sensor output, this sensor is felt to be virtually unusable for sensing atmospheric pressure, and particularly changes in atmospheric pressure.

6.3.3 Temperature Tests

The temperature test results are shown in figure A-15. Known outputs at the end points of guaranteed accurate measurements are -5 V at -45°C and +5 V at +75°C. The figure shows that all measured outputs are below the mean expected value line. Error analysis shows a mean error of 2.70 percent (based on population). Table 2 is a tabulation of measured values with linear expected values and percent error of each measured value indicated.

6.3.4 Field Wind Measurements

The field measurements of windspeed measured by the test instrument compared to a research-grade anemometer are shown in figures A-16 through A-19. As can be seen, correlation is indicated.

7. CONCLUSIONS

The series 200 wind sensor, with the optional temperature and pressure sensors incorporated, is a rugged sensor unit capable of field operation without degradation that could be attributed to "handling conditions." The wind sensor operated effectively at higher windspeeds but suffered a lack of accuracy at the lower windspeeds (less than 5 m/s). However, by proper circuit design, utilizing microprocessor technology and connecting the windspeed output as address lines to an addressable nonvolatile memory containing "true" values, the system can be used effectively.

Using a 10-bit A/D conversion scheme, resolution of parameters are:

Windspeed:	± 0.049 m/s
Wind direction:	± 0.7 deg
Temperature:	± 0.23°C
Pressure:	± 0.0266 psia or ≈ 1.9 mbar MSL

A 12-bit scheme will yield:

Windspeed:	± 0.0122 m/s
Wind direction:	± 0.176 deg
Temperature:	± 0.059°C
Pressure:	± 0.0067 psia or 0.46 mbar MSL

assuming no other system transfer losses.

TABLE 2. MEASURED AND LINEAR EXPECTED VALUES AND PERCENT ERROR OF MEASURED VALUE

Temp °C	Linear Expected	Measured	Difference	Percent Error
-45.23	-5.019	-5.004	+0.015	0.15
-42.15	-4.762	-4.849	-0.087	0.87
-39.51	-4.540	-4.791	-0.251	2.51
-39.06	-4.503	-4.774	-0.271	2.71
-38.61	-4.466	-4.725	-0.259	2.59
-36.62	-4.303	-4.614	-0.311	3.11
-36.38	-4.283	-4.591	-0.308	3.08
-36.27	-4.274	-4.556	-0.282	2.82
-34.30	-4.111	-4.421	-0.310	3.10
-34.06	-4.091	-4.383	-0.292	2.92
-30.79	-3.816	-4.169	-0.353	3.53
-30.72	-3.810	-4.159	-0.349	3.49
-24.71	-3.306	-3.740	-0.434	4.34
-24.01	-3.249	-3.722	-0.473	4.73
-20.30	-2.945	-3.461	-0.516	5.16
-20.07	-2.926	-3.402	-0.476	4.76
-20.01	-2.921	-3.342	-0.421	4.21
-15.58	-2.549	-3.030	-0.481	4.81
-15.25	-2.521	-2.960	-0.439	4.39
-15.17	-2.514	-2.930	-0.416	4.16
-12.30	-2.273	-2.724	-0.451	4.51
-12.25	-2.269	-2.713	-0.444	4.44
-7.72	-1.893	-2.344	-0.451	4.51
7.63	-1.886	-2.308	-0.422	4.22
-2.75	-1.481	-1.589	-0.108	1.08
-1.83	-1.404	-1.552	0.148	1.48
-0.84	-1.321	-1.445	-0.124	1.24
1.22	-1.148	-1.313	-0.165	1.65
5.47	-0.791	-1.006	-0.215	2.15
11.22	-0.386	-0.566	-0.180	1.80
16.42	-0.081	-0.004	+0.077	0.77
19.15	0.301	0.261	-0.040	0.40
21.61	0.552	0.444	-0.108	1.08
22.10	0.592	0.454	-0.138	1.38
22.42	0.618	0.476	-0.142	1.42
23.10	0.674	0.530	-0.144	1.44
23.47	0.705	0.564	-0.141	1.41
26.26	0.936	0.770	-0.166	1.66
28.12	1.092	0.933	-0.159	1.59
34.90	1.662	1.367	-0.295	2.95
39.61	2.048	1.730	-0.318	3.18
44.58	2.465	2.111	-0.354	3.54
56.36	3.444	2.958	-0.486	4.86
62.99	3.999	3.763	-0.236	2.36
68.55	4.463	4.355	-0.108	1.08
75.61	5.051	5.002	-0.049	0.49

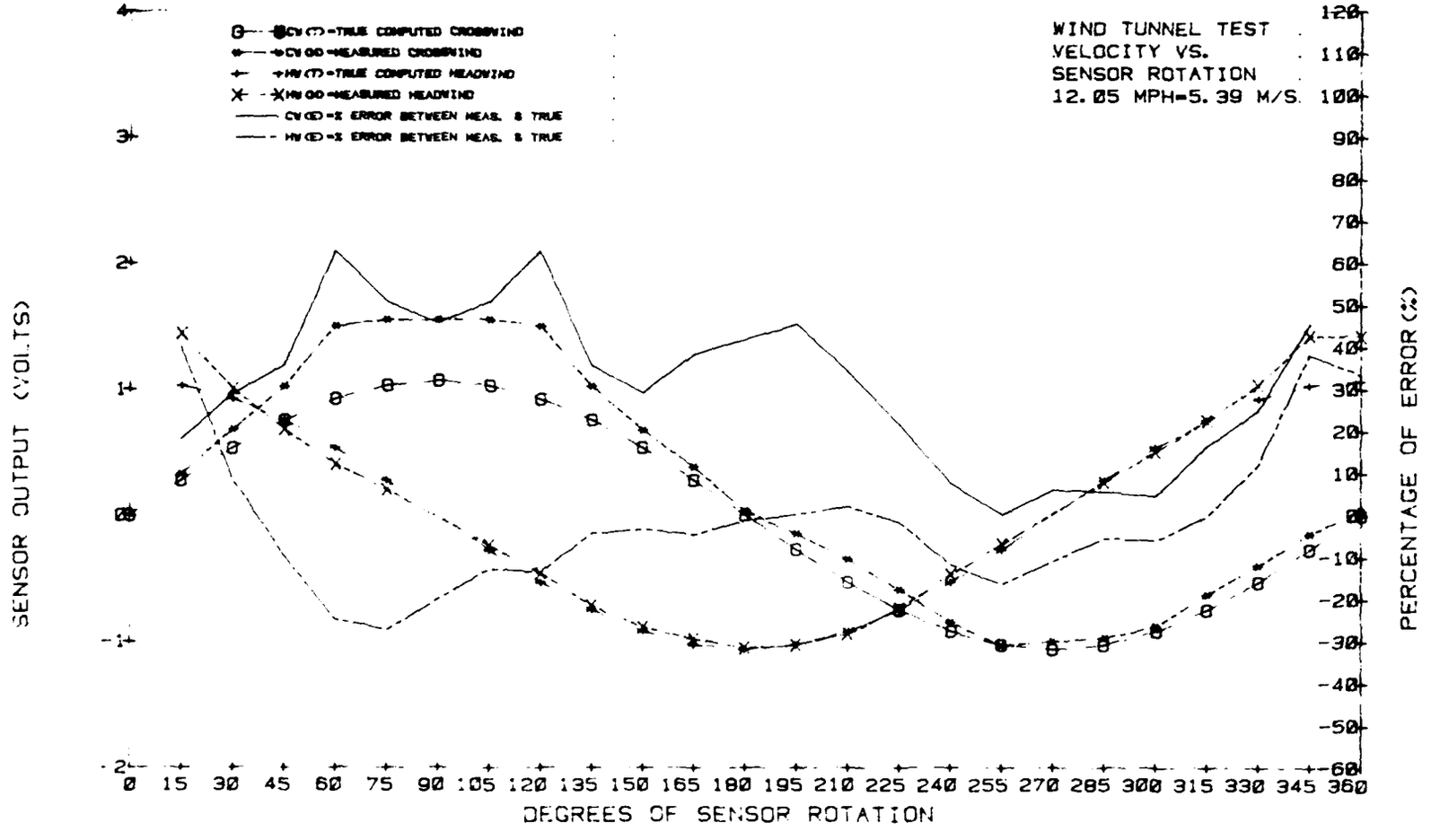

Figure A-1. Wind tunnel test results at 12 mi/h.

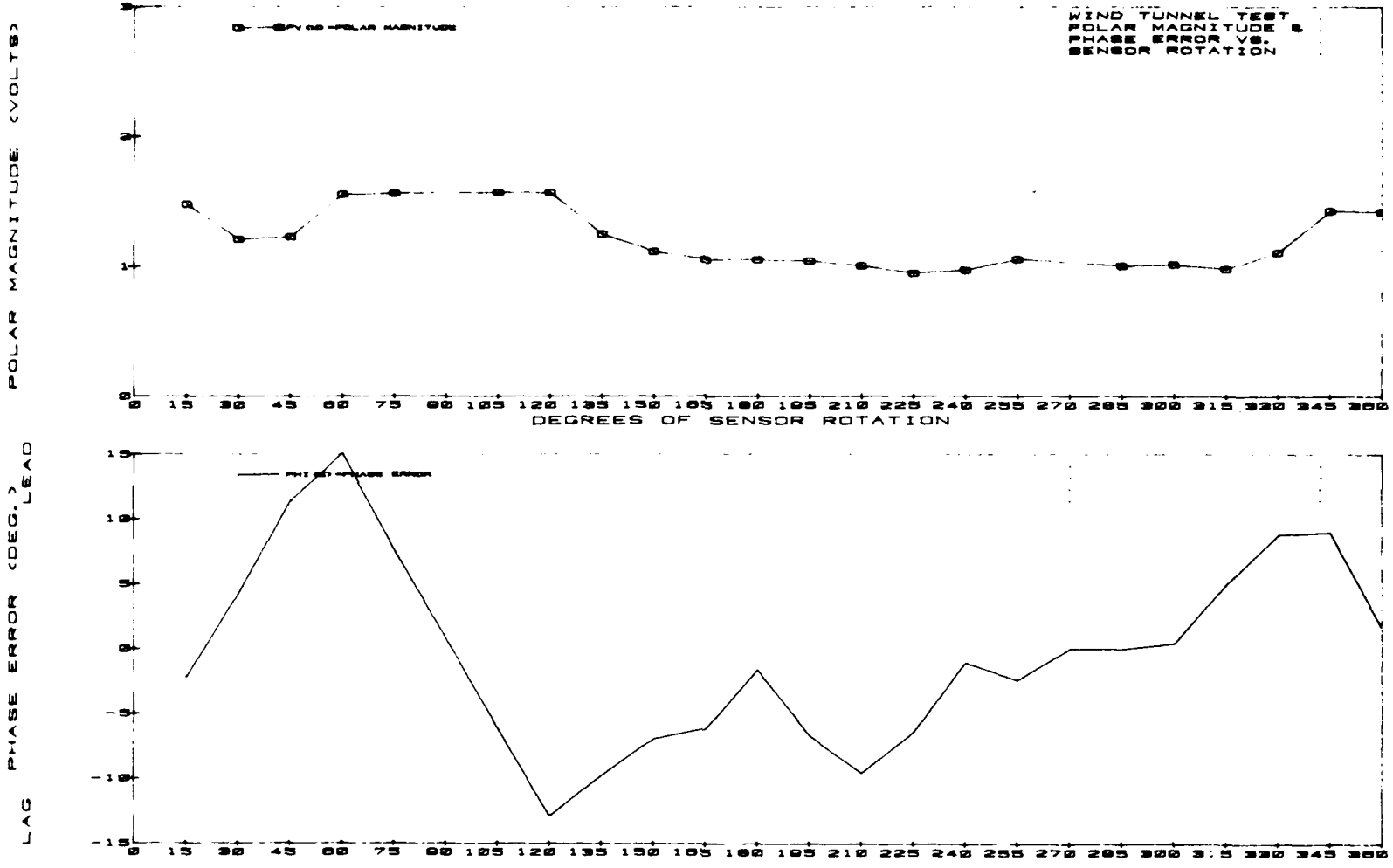

Figure A-2. Wind tunnel test results at 12 mi/h.

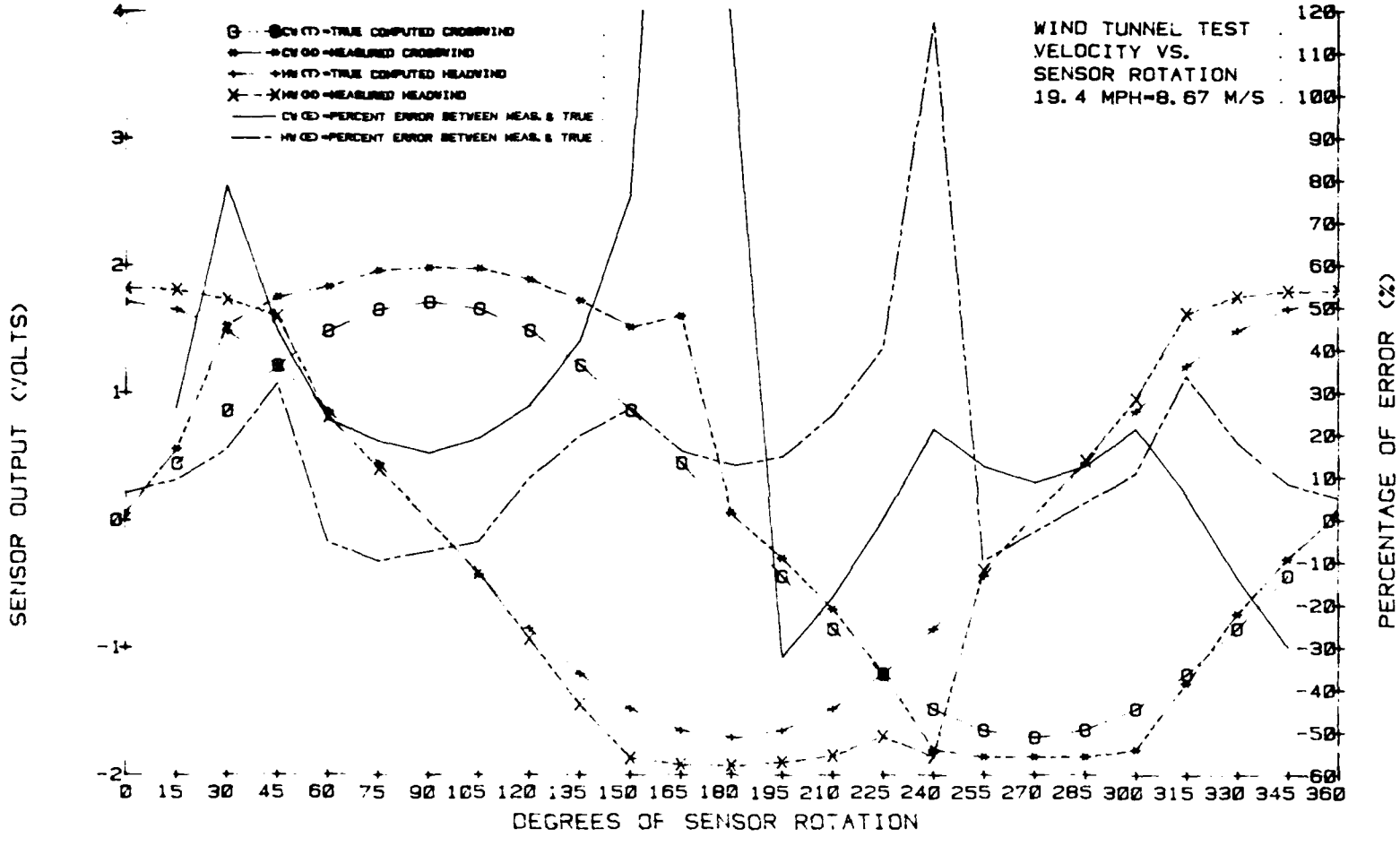

Figure A-3. Wind tunnel test results at 20 mi/h.

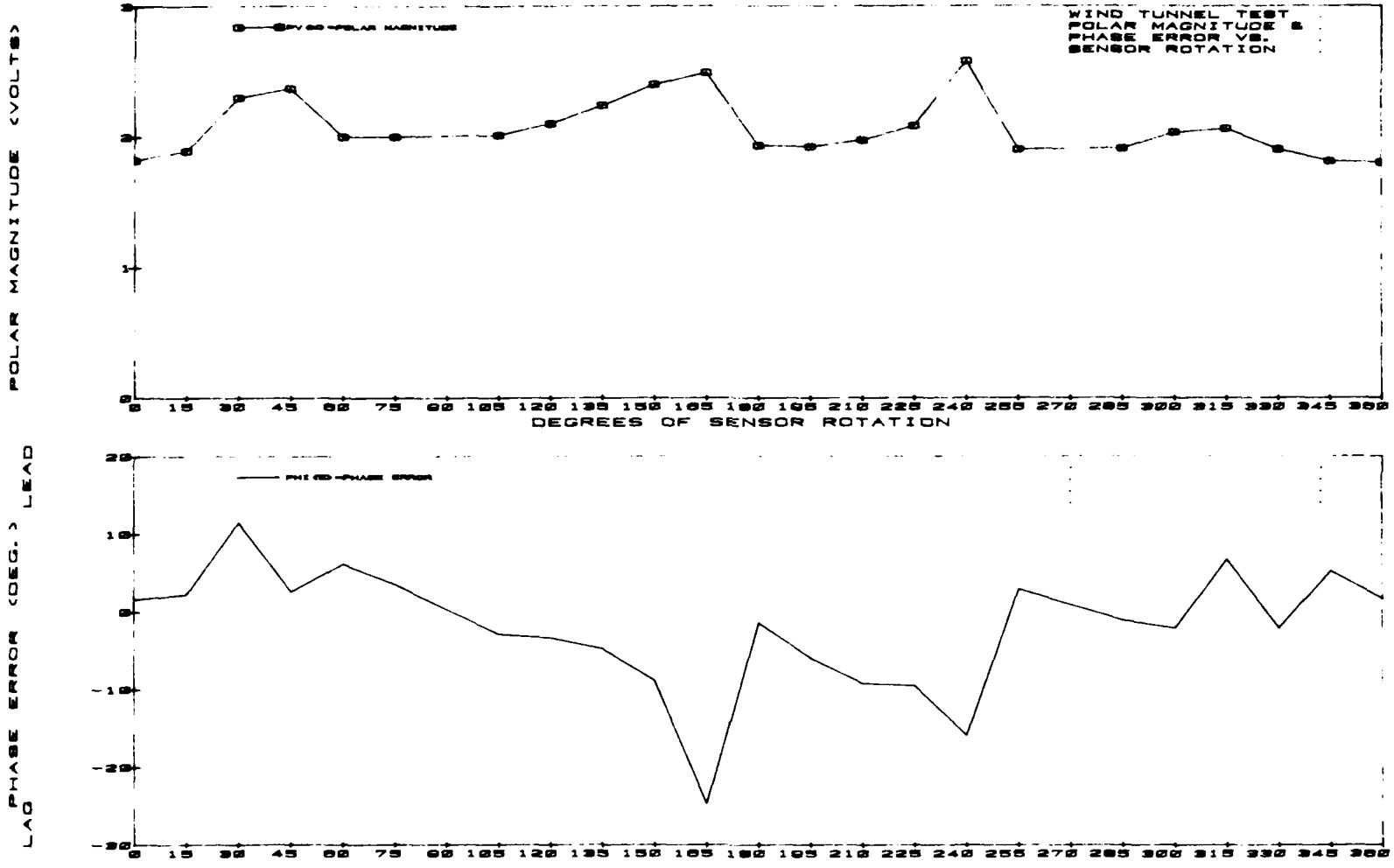

Figure A-4. Wind tunnel test results at 20 mi/h.

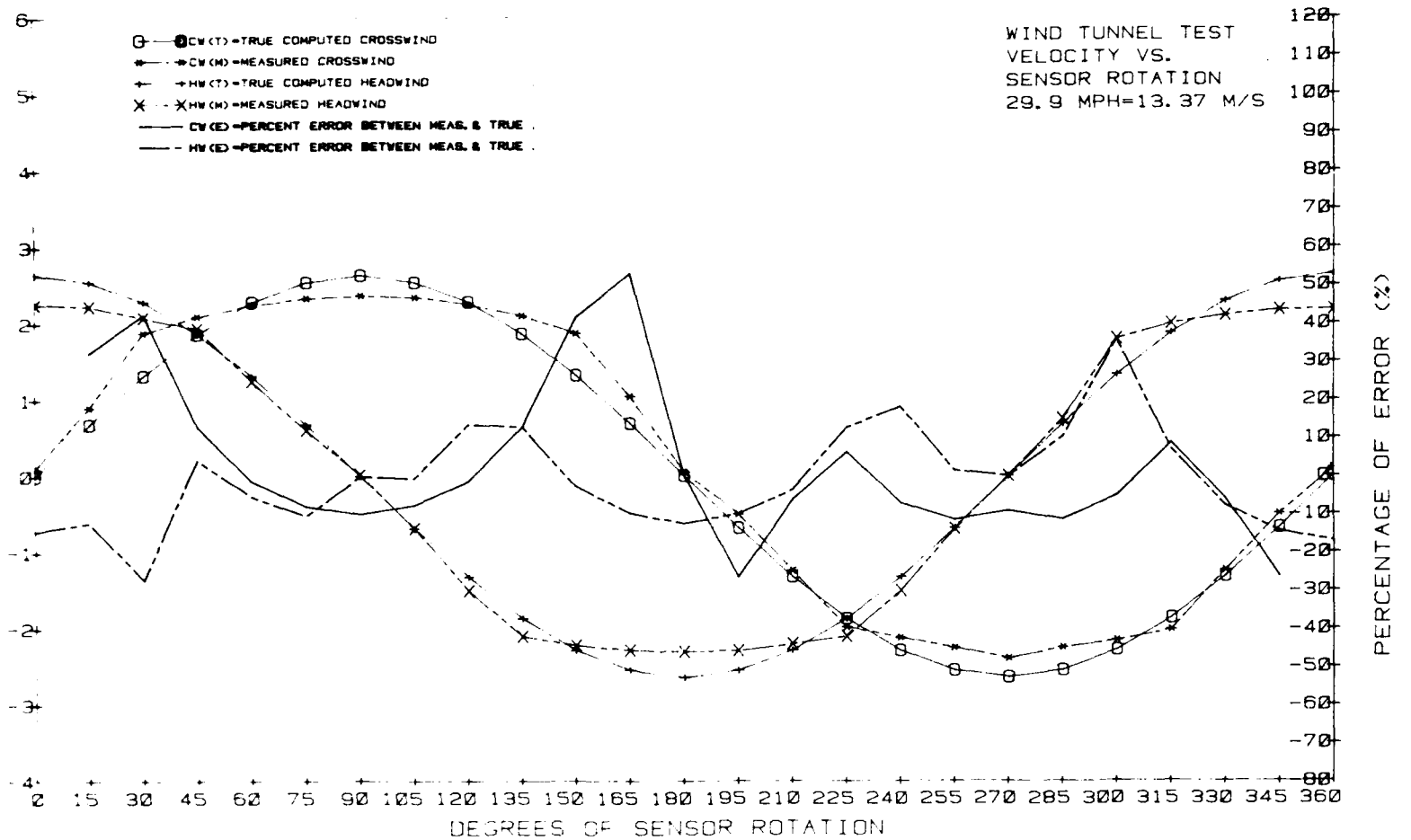

Figure A-5. Wind tunnel test results at 30 mi/h.

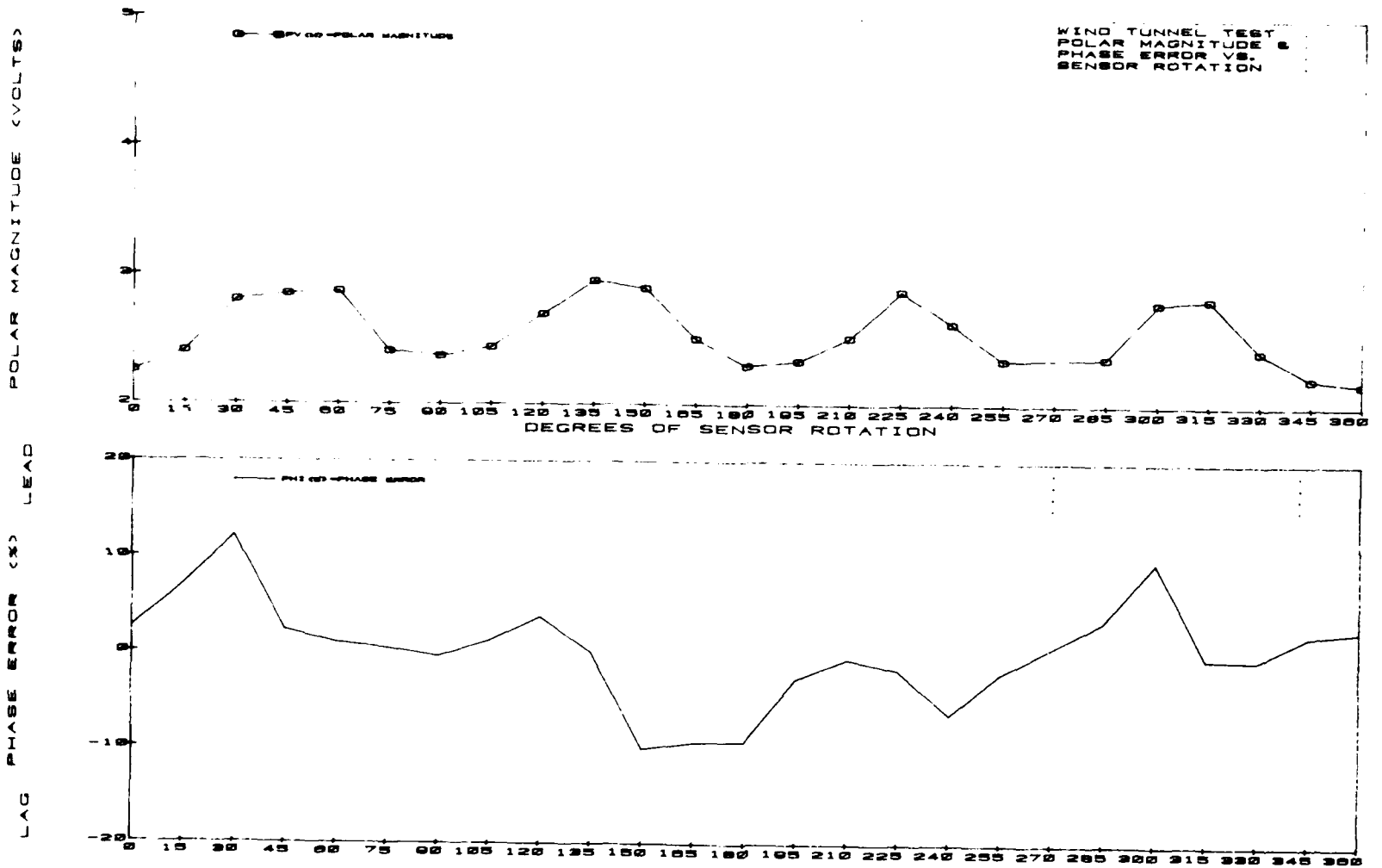

Figure A-6. Wind tunnel test results at 30 mi/h.

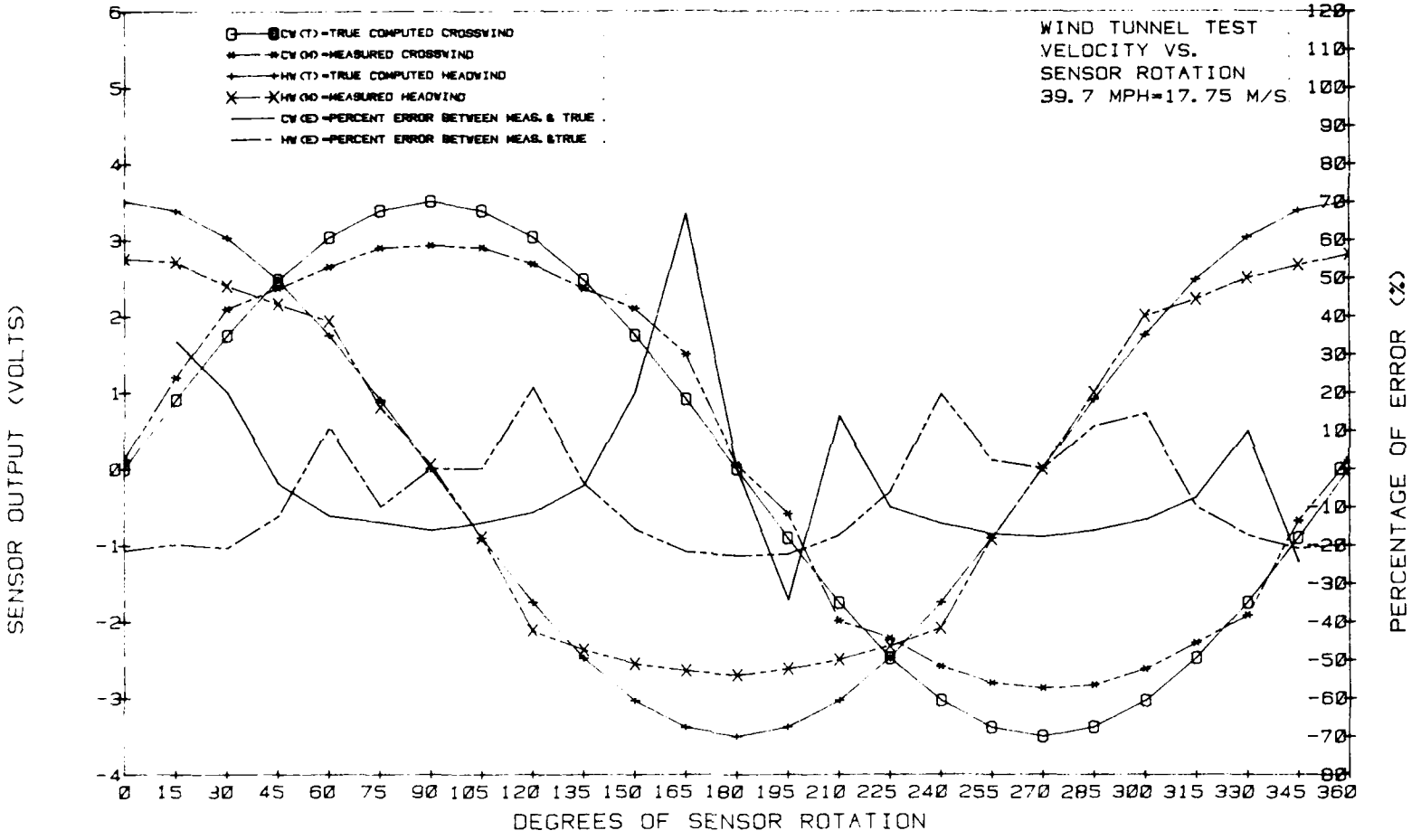

Figure A-7. Wind tunnel test results at 40 mi/h.

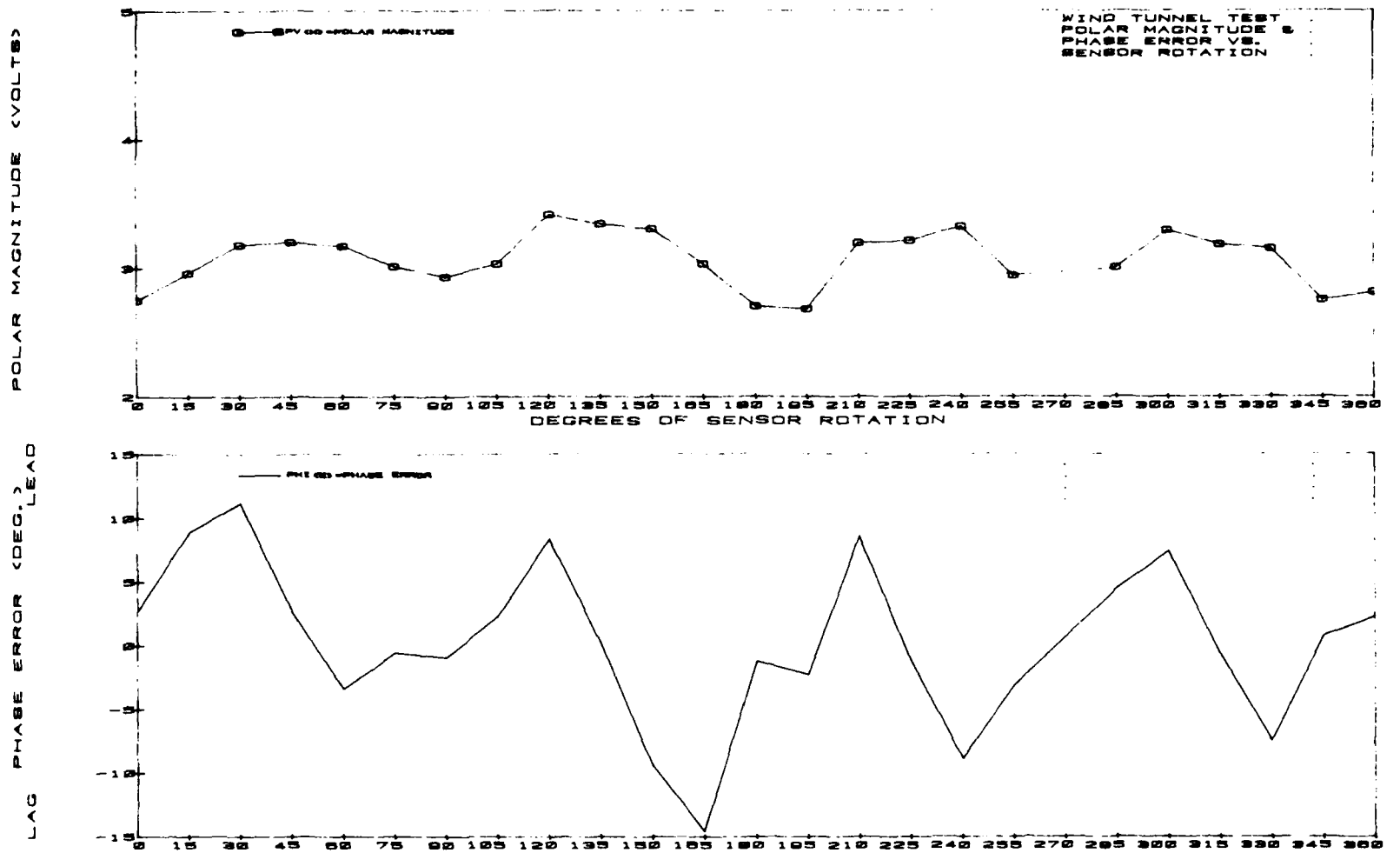

Figure A-8. Wind tunnel test results at 40 mi/h.

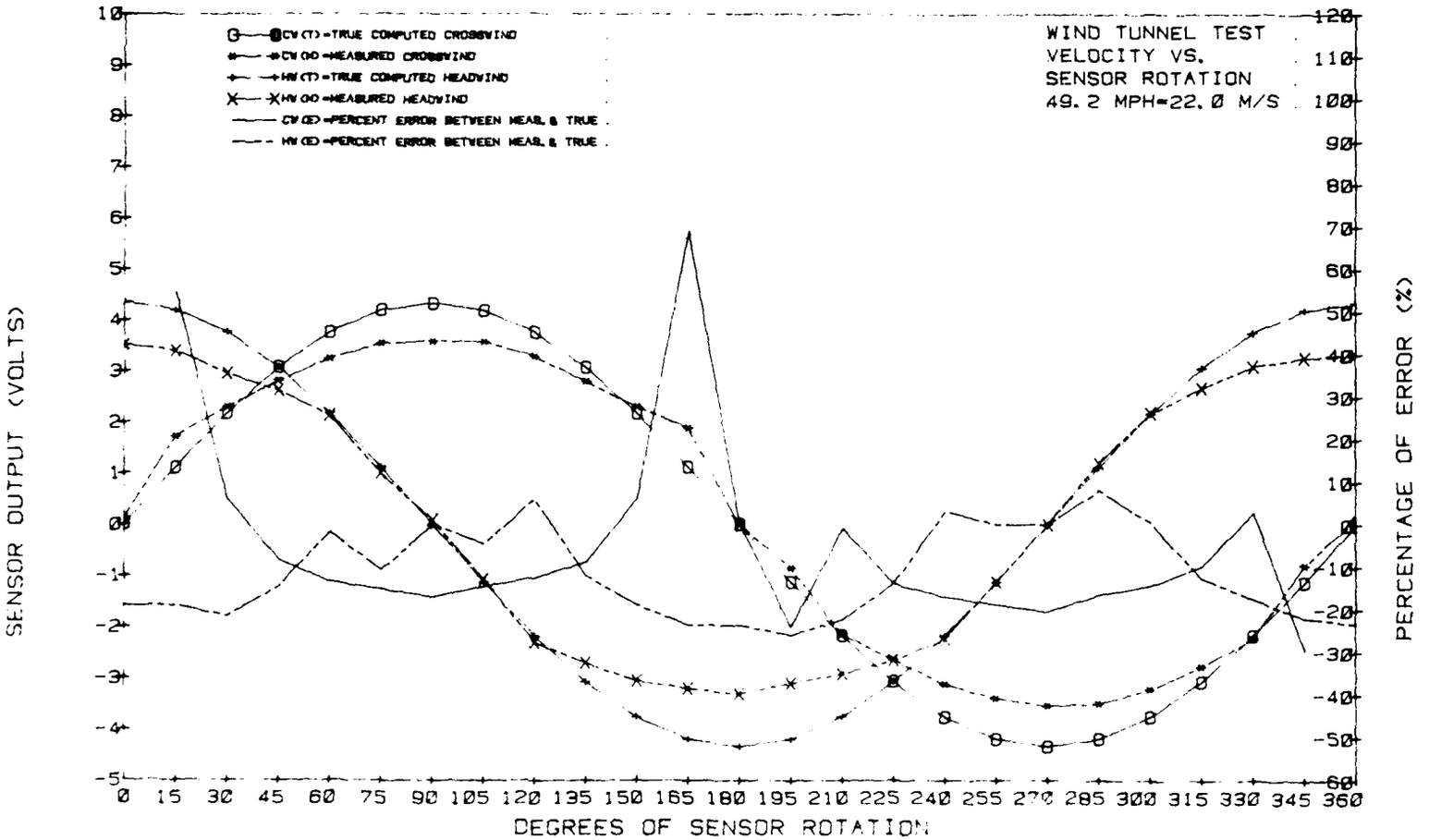

Figure A-9. Wind tunnel test results at 50 mi/h.

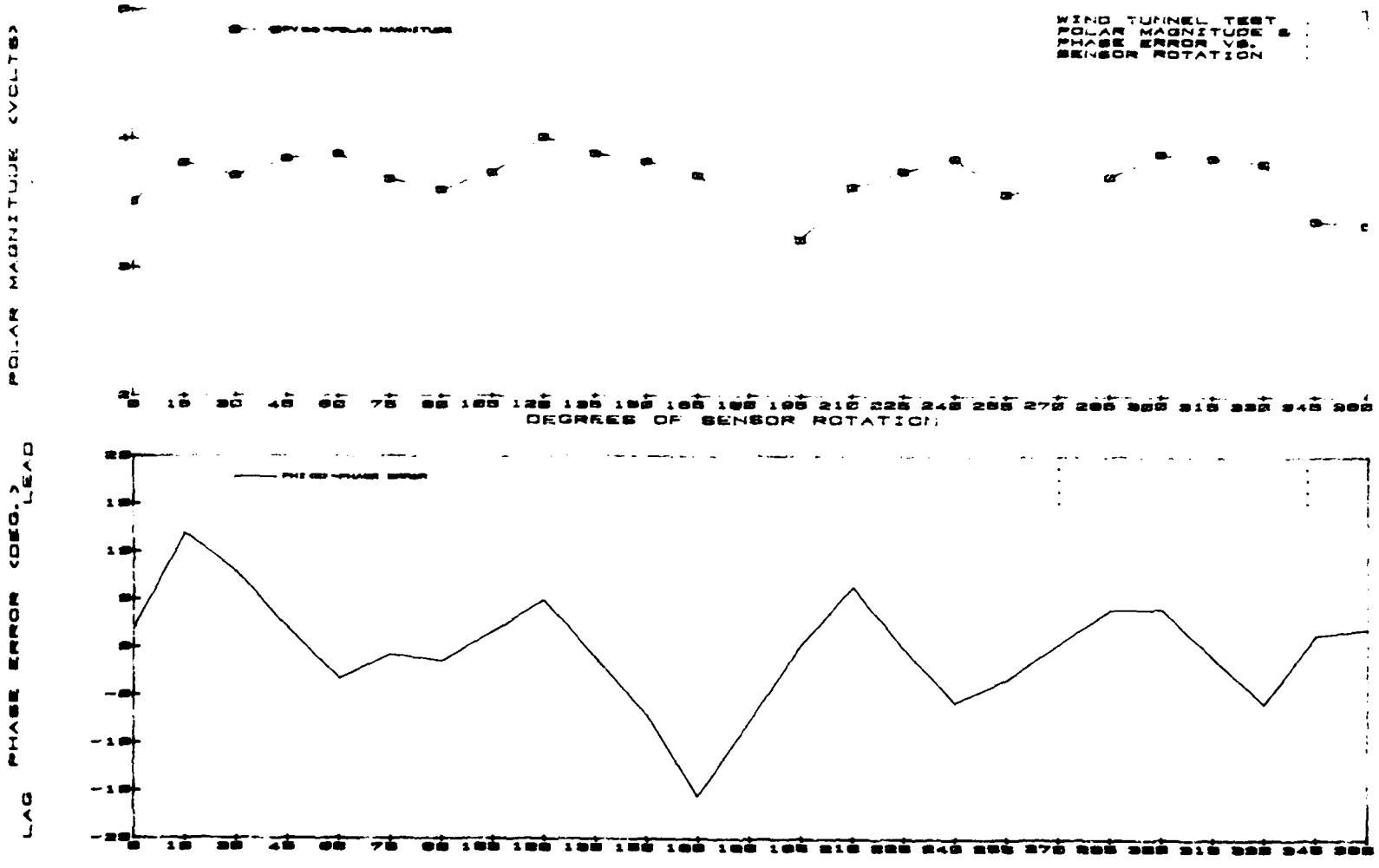

Figure A-10. Wind tunnel test results at 50 mi/h.

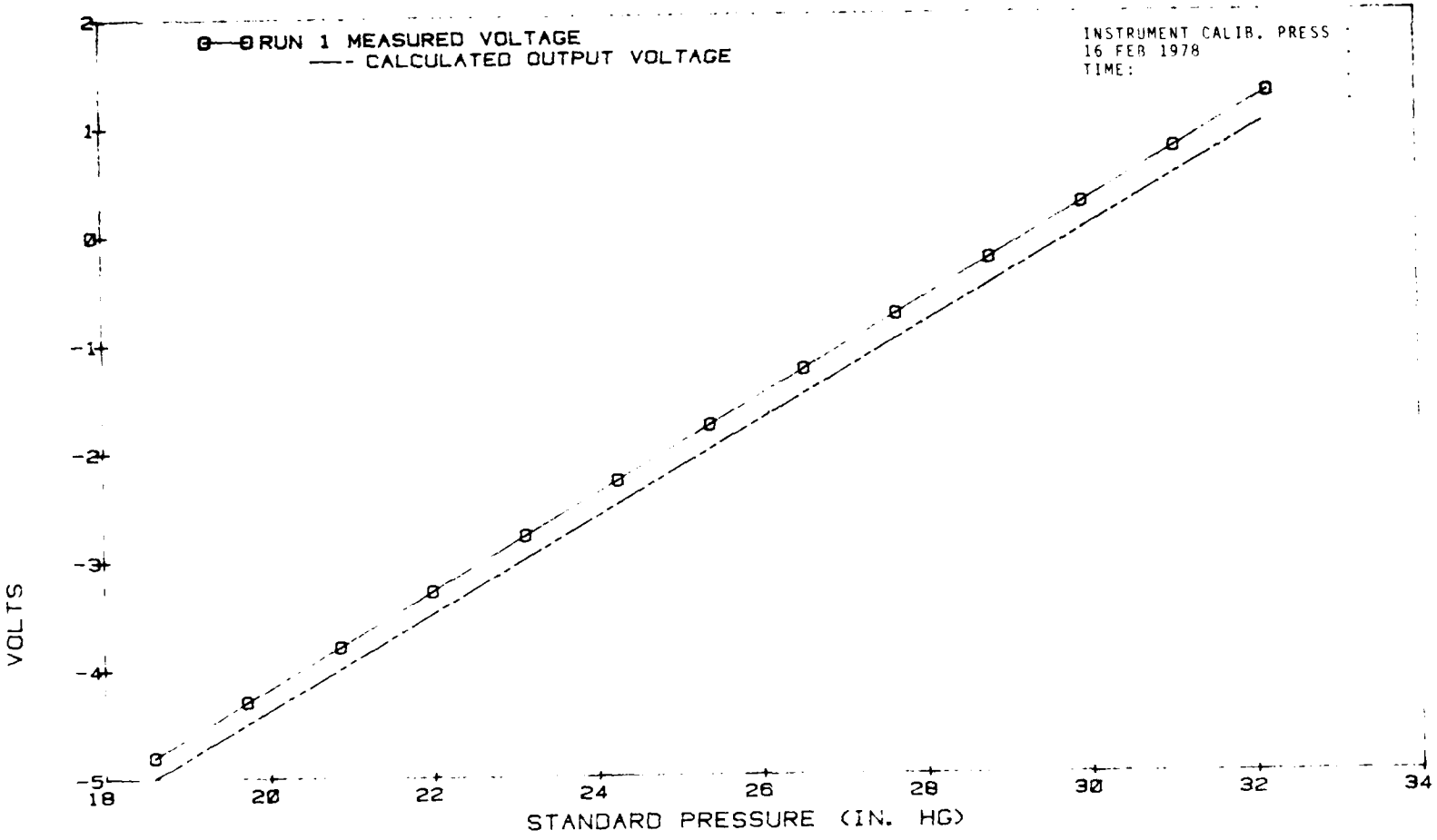

Figure A-11. Pressure test, run 1 (increasing pressure).

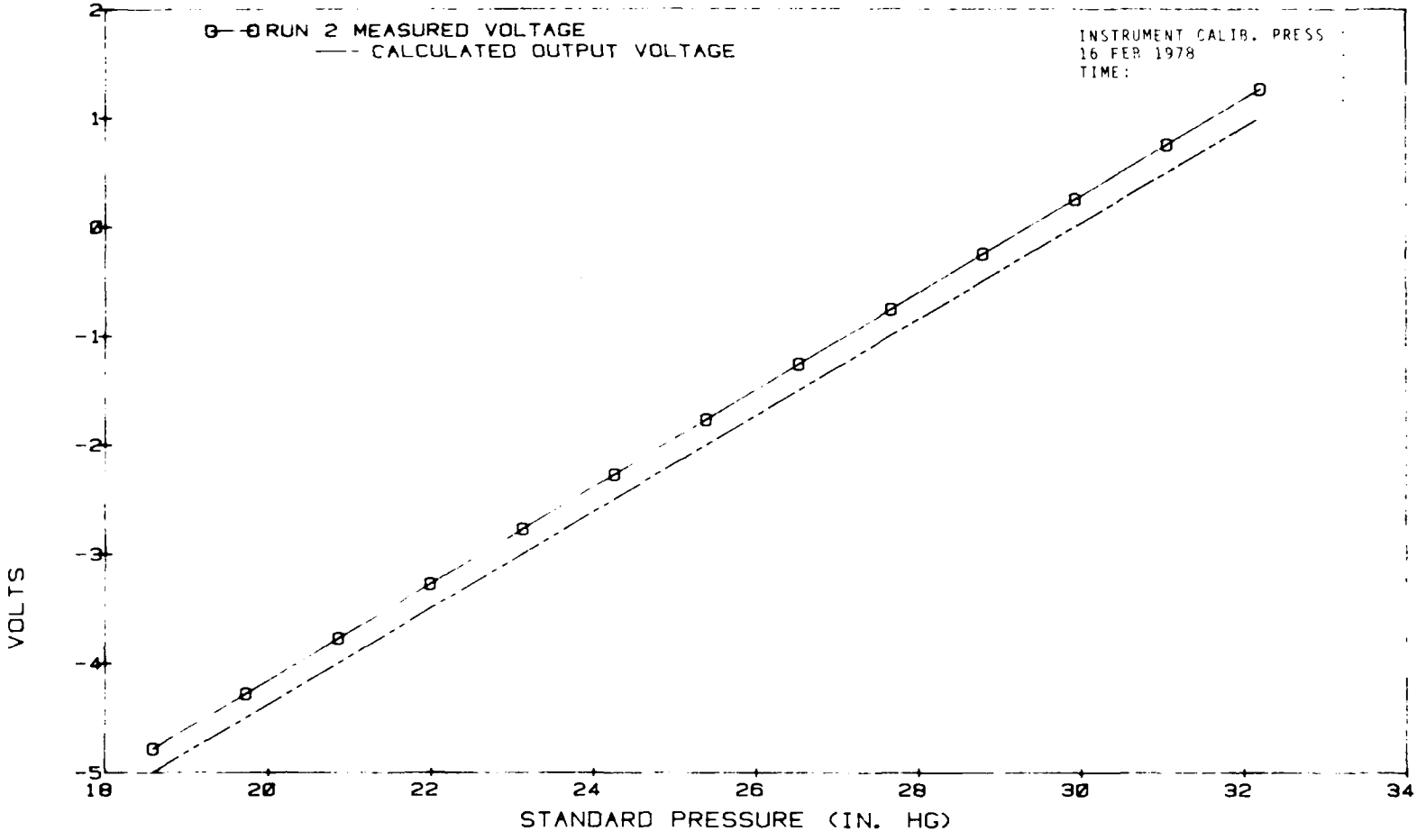

Figure A-12. Pressure test, run 2 (decreasing pressure).

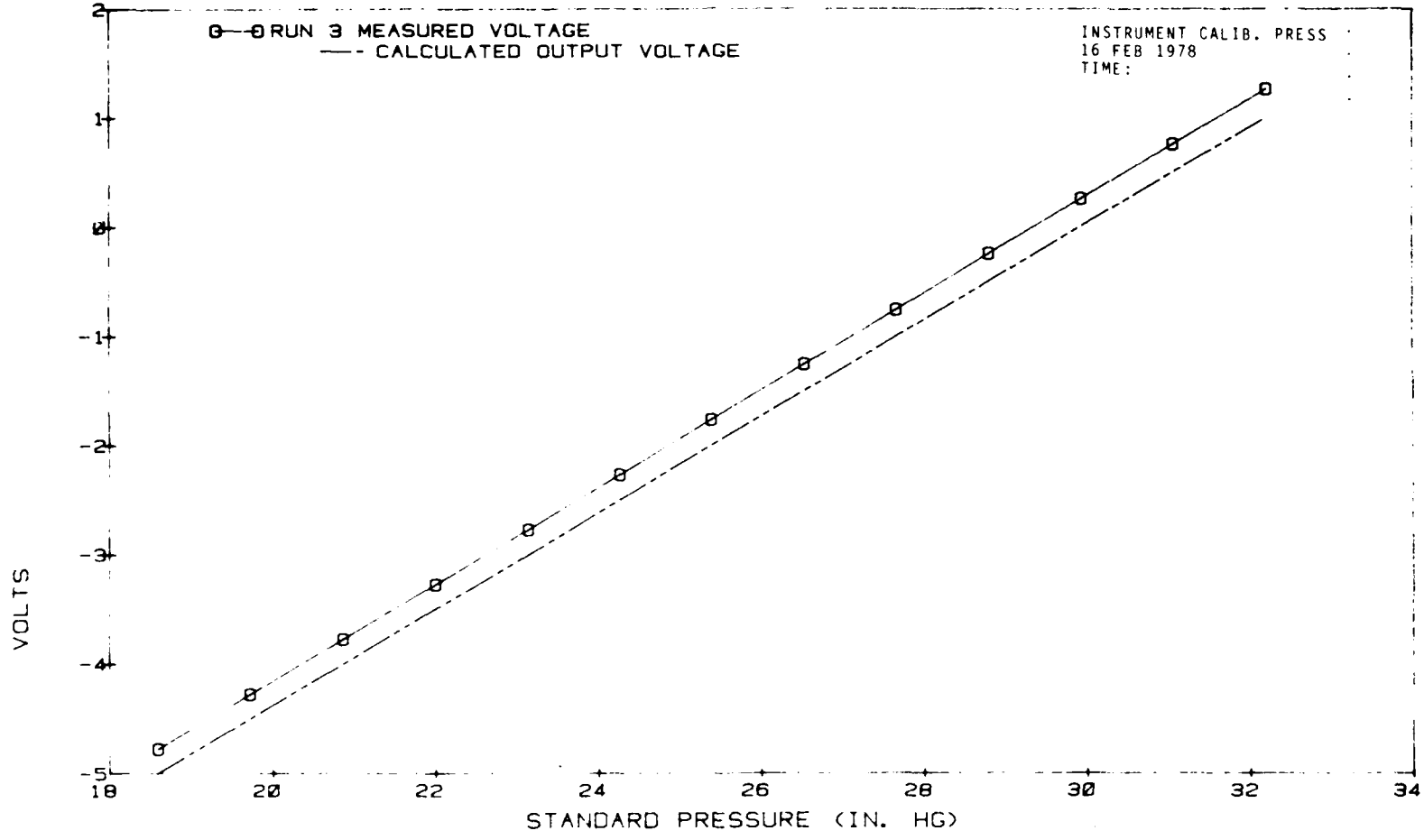

Figure A-13. Pressure test, run 3 (increasing pressure).

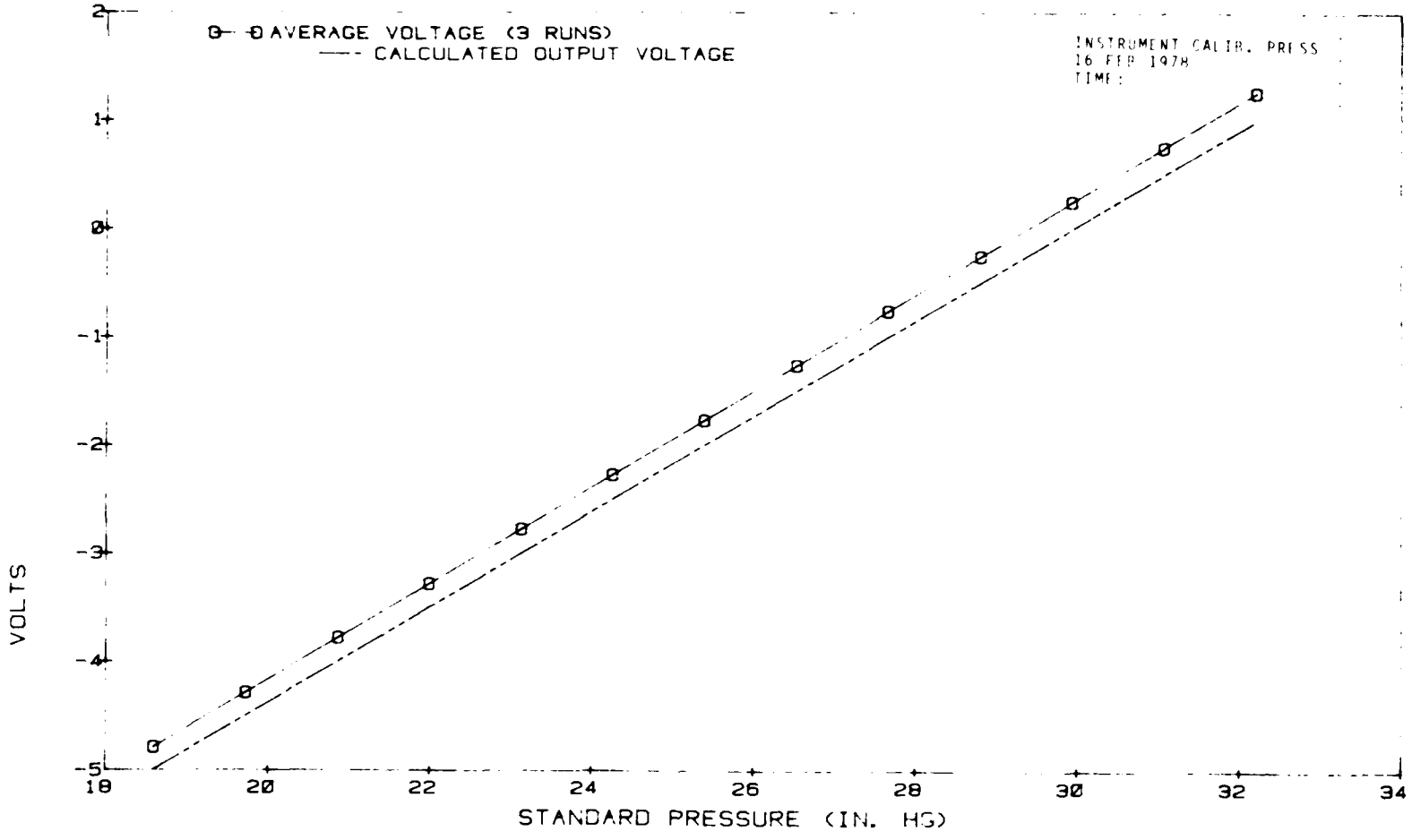

Figure A-14. Pressure test (average of 3 runs).

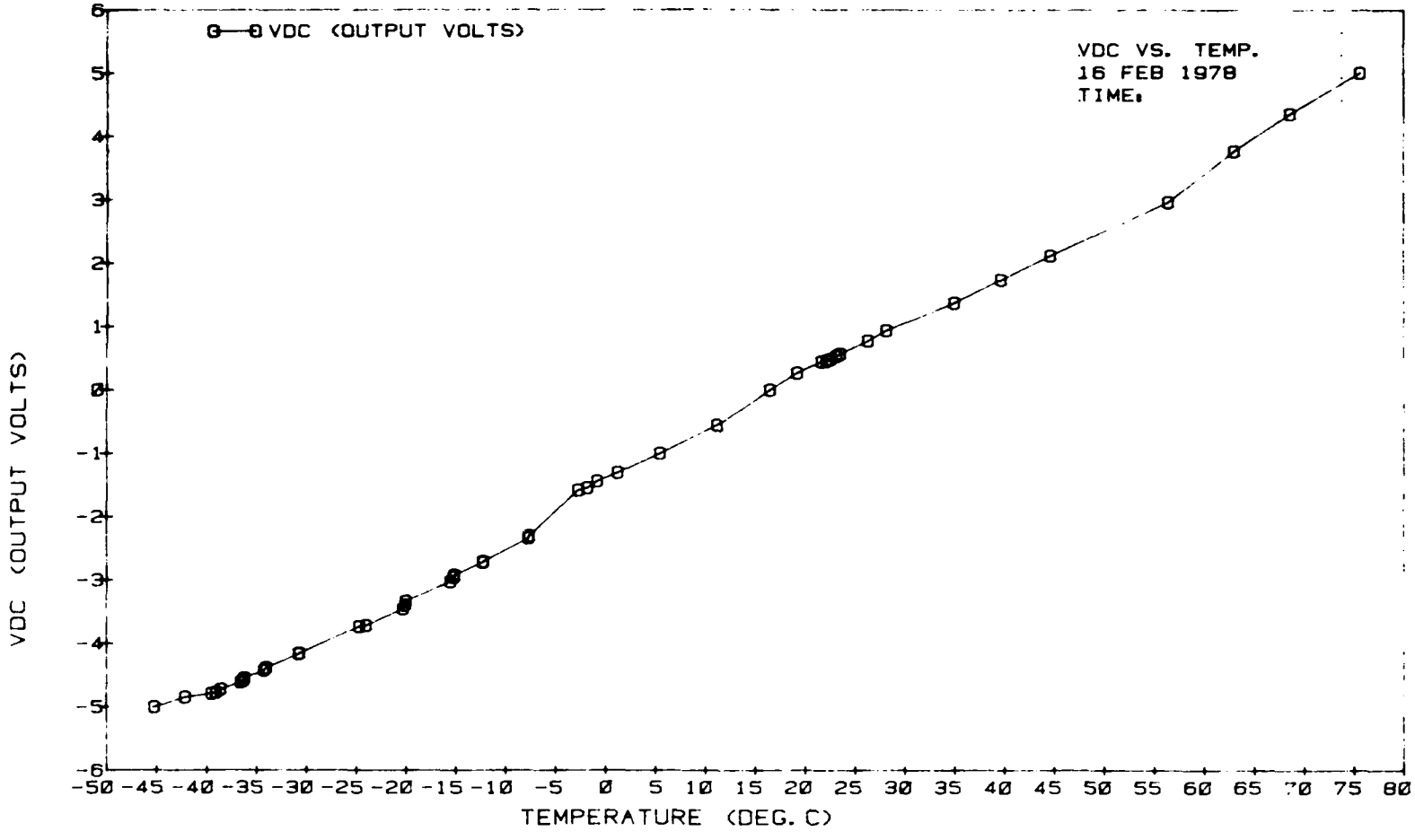

Figure A-15. Temperature test.

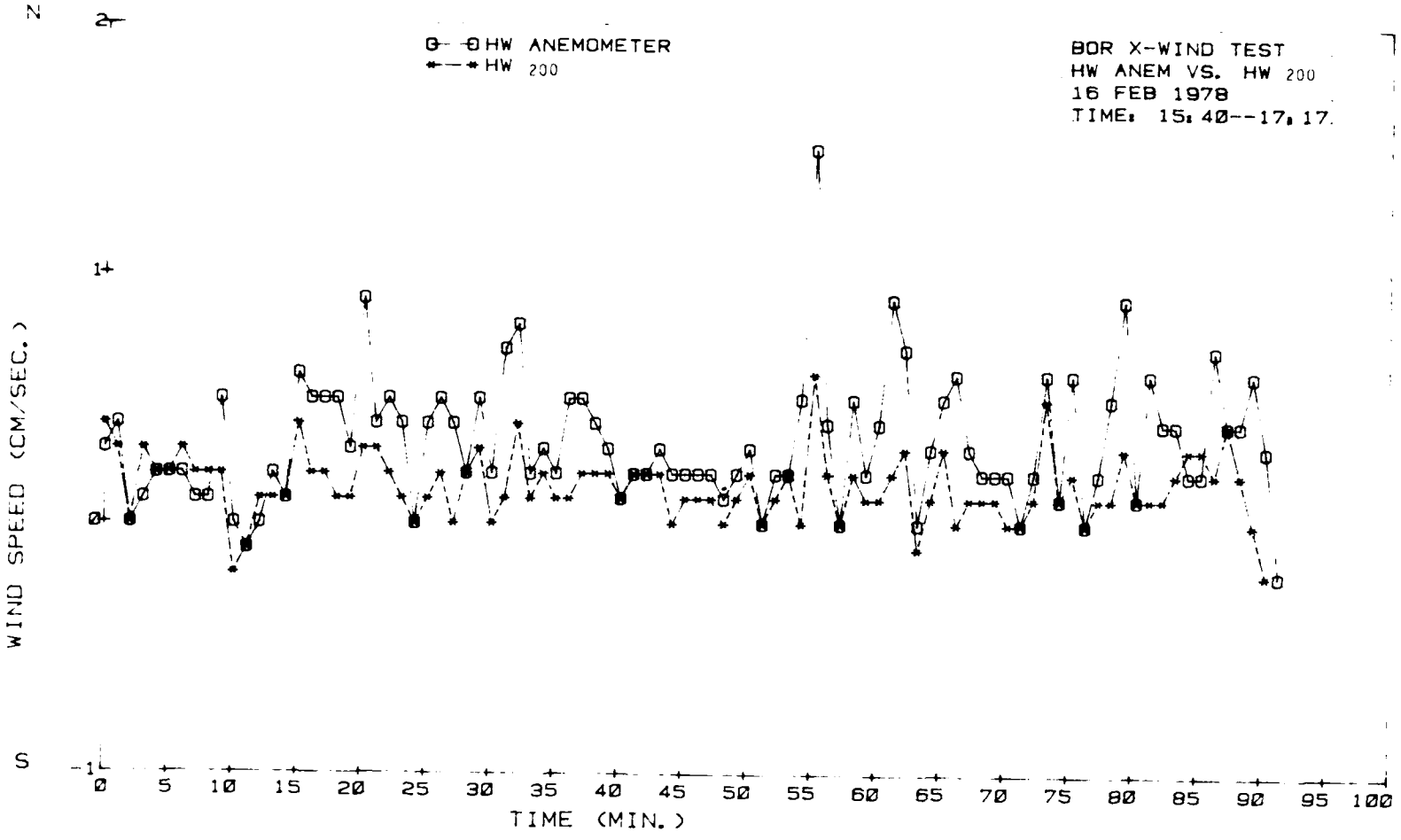

Figure A-16. Field comparison tests, run 1 (headwind).

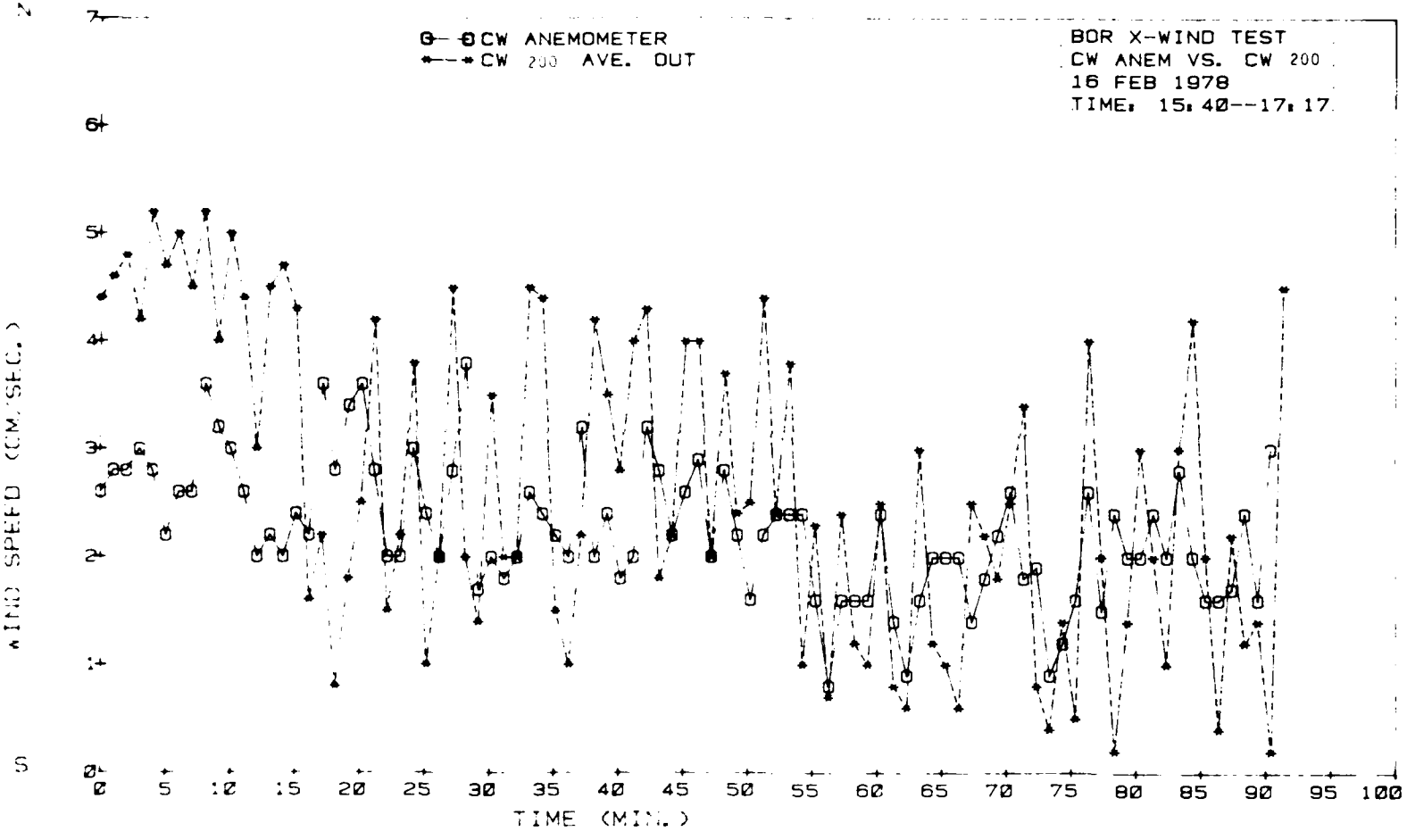

Figure A-17. Field comparison tests, run 1 (crosswind).

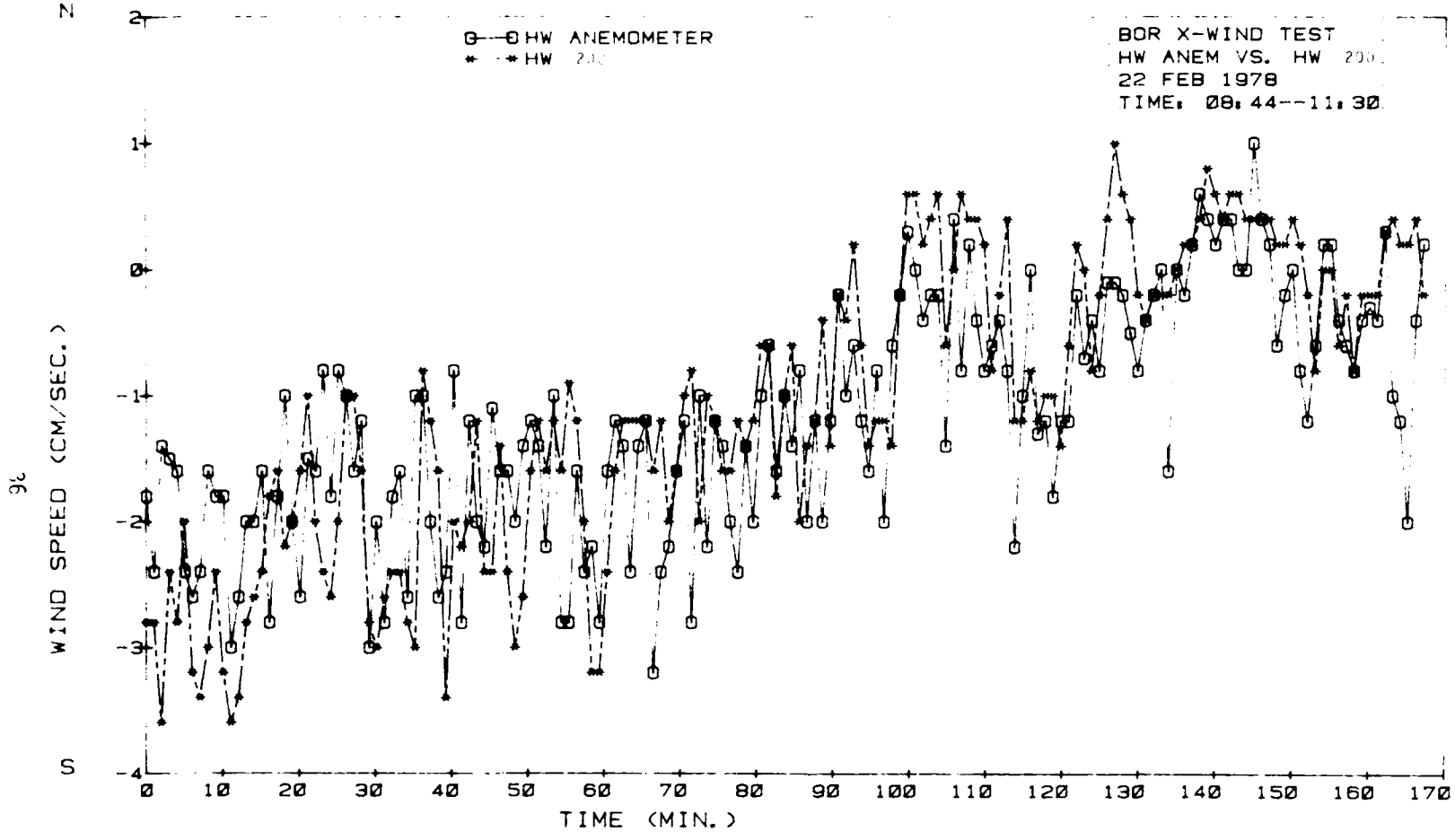

Figure A-18. Field comparison tests, run 2 (headwind).

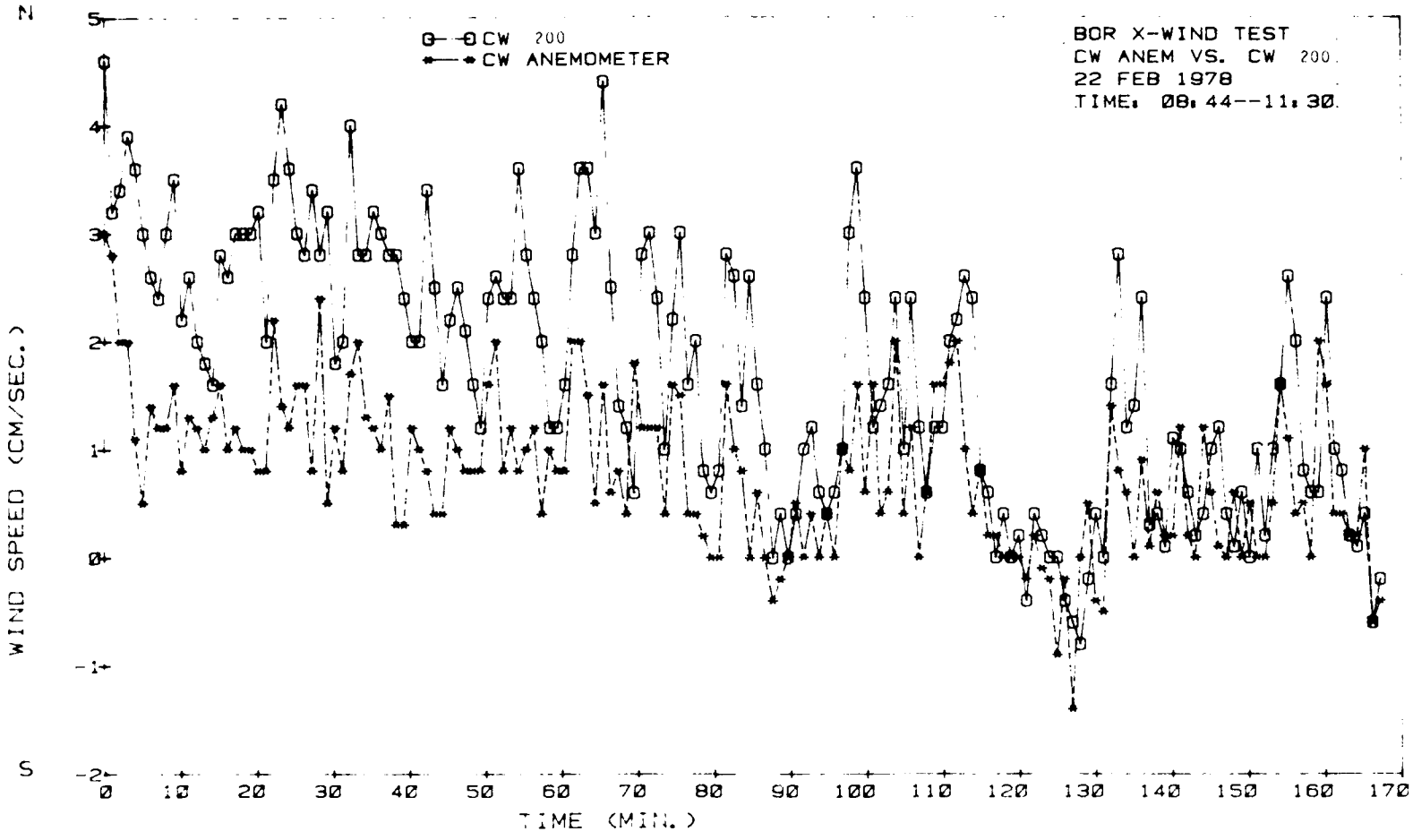

Figure A-19. Field comparison tests, run 2 (crosswind).

APPENDIX B
DAILY WEATHER PARAMETERS FEBRUARY 1980

Day	Temp (^{O}F)						Avg	Winds				
Feb								Fastest		Peak Gust		
78	Max	Min	Avg	Dep	From	Norm	Speed	mi/h	Dir	mi/h	Dir	Time
16	55	35	45		-4		14.7	28	300^{O}	44	NW	1954
22	63	29	46		-4		3.1	9	010^{O}	12	SW	1306

DISTRIBUTION LIST

Commander
US Army Aviation Center
ATTN: ATZQ-D-MA
Fort Rucker, AL 36362

Chief, Atmospheric Sciences Div
Code ES-81
NASA
Marshall Space Flight Center, AL 35812

Commander
US Army Missile Command
ATTN: DRDMI-RRA/Dr.O. M. Essenwanger
Redstone Arsenal, AL 35809

Commander
US Army Missile Command
ATTN: DRSMI-OG (B. W. Fowler)
Redstone Arsenal, AL 35809

Commander
US Army Missile R&D Command
ATTN: DRDMI-TEM (R. Haraway)
Redstone Arsenal, AL 35809

Redstone Scientific Information Center
ATTN: DRSMI-RPRD (Documents)
US Army Missile Command
Redstone Arsenal, AL 35809

Commander
HQ, Fort Huachuca
ATTN: Tech Ref Div
Fort Huachuca, AZ 85613

Commander
US Army Intelligence
Center & School
ATTN: ATSI-CD-MD
Fort Huachuca, AZ 85613

Commander
US Army Yuma Proving Ground
ATTN: Technical Library
Bldg 2105
Yuma, AZ 85364

Dr. Frank D. Eaton
Geophysical Institute
University of Alaska
Fairbanks, AK 99701

Naval Weapons Center
Code 3918
ATTN: Dr. A. Shlanta
China Lake, CA 93555

Commanding Officer
Naval Envir Prediction Rsch Facility
ATTN; Library
Monterey, CA 93940

Sylvania Elec Sys Western Div
ATTN: Technical Reports Lib
PO Box 205
Mountain View, CA 94040

Geophysics Officer
PMTC Code 3250
Pacific Missile Test Center
Point Mugu, CA 93042

Commander
Naval Ocean Systems Center
(Code 4473)
ATTN: Technical Library
San Diego, CA 92152

Meteorologist in Charge
Kwajalein Missile Range
PO Box 67
APO San Francisco, CA 96555

Director
NOAA/ERL/APCL R31
RB3-Room 567
Boulder, CO 80302

Dr.B. A. Silverman D-1200
Office of Atmos Resources Management
Water and Power Resources Service
PO Box 25007Denver Federal Center, Bldg. 67
Denver, CO 80225

Hugh W. Albers (Executive Secretary)
CAO Subcommittee on Atmos Rsch
National Science Foundation Room 510
Washington, DC 2055

Dr. Eugene W. Bierly
Director, Division of Atmos Sciences
National Scinece Foundation
1800 G Street, N.W.
Washington, DC 20550

Commanding Officer
Naval Research Laboratory
Code 2627
Washington, DC 20375

Defense Communications Agency
Technical Library Center
Code 222
Washington, DC 20305

Director
Naval Research Laboratory
Code 5530
Washington, DC 20375

Dr. J. M. MacCallum
Naval Research Laboratory
Code 1409
Washington, DC 20375

HQDA (DAEN-RDM/Dr. de Percin)
Washington, DC 20314

The Library of Congress
ATTN: Exchange & Gift Div
Washington, DC 20540
2

Mil Asst for Atmos Sci Ofc of
the Undersecretary of Defense
for Rsch & Engr/E&LS - RM 3D129
The Pentagon
Washington, DC 20301

AFATL/DLODL
Technical Library
Eglin AFB, FL 32542

Naval Training Equipment Center
ATTN: Technical Information Center
Orlando, FL 32813

Technical Library
Chemical Systems Laboratory
Aberdeen Proving Ground, MD 21010

US Army Materiel Systems
Analysis Activity
ATTN: DRXSY-MP
APG, MD 21005

Commander
ERADCOM
ATTN: DRDEL-PA/ILS/-ED
2800 Powder Mill Road
Adelphi, MD 20783

Commander
ERADCOM
ATTN: DRDEL-ST-T (Dr. B. Zarwyn)
2800 Powder Mill Road
Adelphi, MD 20783
02

Commander
Harry Diamond Laboratories
ATTN: DELHD-CO
2800 Powder Mill Road
Adelphi, MD 20783

Chief
Intel Mat Dev & Spt Ofc
ATTN: DELEW-WL-I
Bldg 4554
Fort George G. Mead, MD 20755

Acquisitions Section, IRDB-D823
Library & Info Svc Div, NOAA
6009 Executive Blvd.
Rockville, MD 20752

Naval Surface Weapons Center
White Oak Library
Silver Spring, MD 20910

Air Force Geophysics Laboratory
ATTN: LCC (A. S. Carten, Jr.)
Hanscom AFB, MA 01731

Air Force Geophysics Laboratory
ATTN: LYD
Hanscom AFB, MA 01731

Meteorology Division
AFGL/LY
Hanscom AFB, MA 01731

The Environmental Research
Institute of MI
ATTN: IRIA Library
PO Box 8618
Ann Arbor, MI 48107

Mr. William A. Main
USDA Forest Service
1407 S. Harrison Road
East Lansing, MI 48823

Dr. A. D. Belmont
Research Division
PO Box 1249
Control Data Corp
Minneapolis, MN 55440

Commander
Naval Oceanography Command
Bay St. Louis, MS 39529

Commanding Officer
US Army Armament R&D Command
ATTN; DRDAR-TSS Bldg 59
Dover, NJ 07801

Commander
ERADCOM Scientific Advisor
ATTN: DRDEL-SA
Fort Monmouth, NJ 07703

Commander
ERADCOM Tech Support Activity
ATTN: DELSD-L
Fort Monmouth, NJ 07703

Commander
HQ, US Army Avionics R&D Actv
ATTN: DAVAA-O
Fort Monmouth, NJ 07703

Commander
USA Elect Warfare Lab
ATTN: DELEW-DA (File Cy)
Fort Monmouth, NJ 07703

Commander
US Army Electronics R&D Command
ATTN: DELCS-S
Fort Monmouth, NJ 07703

Commander
US Army Satellite Comm Agency
ATTN: DRCPM-SC-3
Fort Monmouth, NJ 07703

Commander/Director
US Army Combat Survl & Target
Acquisition Laboratory
ATTN: DELCS-D
Fort Monmouth, NJ 07703

Director
Night Vision & Electro-Optics Laboratory
ATTN: DELNV-L (Dr. R. Buser)
Fort Belvoir, VA 22060

Project Manager, FIREFINDER
ATTN: DRCPM-FF
Fort Monmouth, NJ 07703

PM, Firefinder/REMBASS
ATTN: DRCPM-FFR-TM
Fort Monmouth, NJ 07703

6585 TG/WE
Holloman AFB, NM 88330

AFWL/Technical Library (SUL)
Kirtland AFB, NM 87117

AFWL/WE
Kirtland, AFB, NM 87117

TRASANA
ATTN: ATAA-SL (D. Anguiano)
WSMR, NM 88002

Commander
US Army White Sands Missile Range
ATTN: STEWS-PT-AL
White Sands Missile Range, NM 88002

Rome Air Development Center
ATTN: Documents Library
TSLD (Bette Smith)
Griffiss AFB, NY 13441

Environmental Protection Agency
Meteorology Laboratory, MD 80
Rsch Triangle Park, NC 27711

US Army Research Office
ATTN: DRXRO-PP
PO Box 12211
Rsch Triangle Park, NC 27709

Commandant
US Army Field Artillery School
ATTN: ATSF-CD-MS (Mr. Farmer)
Fort Sill, OK 73503

Commandant
US Army Field Artillery School
ATTN: ATSF-CF-R
Fort Sill, OK 73503

Commandant
US Army Field Artillery School
ATTN: Morris Swett Library
Fort Sill, OK 73503

Commander
US Army Dugway Proving Ground
ATTN: STEDP-MT-DA-M
(Mr. Paul Carlson)
Dugway, UT 84022

Commander
US Army Dugway Proving Ground
ATTN: MT-DA-L
Dugway, UT 84022

US Army Dugway Proving Ground
ATTN: STEDP-MT-DA-T
(Dr. W. A. Peterson)
Dugway, UT 84022

Inge Dirmhirn, Professor
Utah State University, UMC 48
Logan, UT 84322

Defense Technical Information Center
ATTN: DTIC-DDA-2
Cameron Station, Bldg. 5
Alexandria, VA 22314
12

Commanding Officer
US Army Foreign Sci & Tech Cen
ATTN: DRXST-IS1
220 7th Street, NE
Charlottesville, VA 22901

Naval Surface Weapons Center
Code G65
Dahlgren, VA 22448

Commander
US Army Night Vision
& Electro-Optics Lab
ATTN: DELNV-D
Fort Belvoir, VA 22060

Commander
USATRADOC
ATTN: ATCD-FA
Fort Monroe, VA 23651

Commander
USATRADOC
ATTN: ATCD-IR
Fort Monroe, VA 23651

Dept of the Air Force
5WW/DN
Langley AFB, VA 23665

US Army Nuclear & Cml Agency
ATTN: MONA-WE
Springfield, VA 22150

Director
US Army Signals Warfare Lab
ATTN: DELSW-OS (Dr. Burkhardt)
Vint Hill Farms Station
Warrenton, VA 22186

Commander
US Army Cold Regions Test Cen
ATTN: STECR-OP-PM
APO Seattle, WA 98733

ATMOSPHERIC SCIENCES RESEARCH PAPERS

1. Lindberg, J.D., "An Improvement to a Method for Measuring the Absorption Coefficient of Atmospheric Dust and other Strongly Absorbing Powders," ECOM-5565, July 1975.
2. Avara, Elton, P., "Mesoscale Wind Shears Derived from Thermal Winds," ECOM-5566, July 1975.
3. Gomez, Richard B., and Joseph H. Pierluissi, "Incomplete Gamma Function Approximation for King's Strong-Line Transmittance Model," ECOM-5567, July 1975.
4. Blanco, A.J., and B.F. Engebos, "Ballistic Wind Weighting Functions for Tank Projectiles," ECOM-5568, August 1975.
5. Taylor, Fredrick J., Jack Smith, and Thomas H. Pries, "Crosswind Measurements through Pattern Recognition Techniques," ECOM-5569, July 1975.
6. Walters, D.L., "Crosswind Weighting Functions for Direct-Fire Projectiles," ECOM-5570, August 1975.
7. Duncan, Louis D., "An Improved Algorithm for the Iterated Minimal Information Solution for Remote Sounding of Temperature," ECOM-5571, August 1975.
8. Robbiani, Raymond L., "Tactical Field Demonstration of Mobile Weather Radar Set AN/TPS-41 at Fort Rucker, Alabama," ECOM-5572, August 1975.
9. Miers, B., G. Blackman, D. Langer, and N. Lorimier, "Analysis of SMS GOES Film Data," ECOM-5573, September 1975.
10. Manquero, Carlos, Louis Duncan, and Rufus Bruce, "An Indication from Satellite Measurements of Atmospheric CO2 Variability," ECOM-5574, September 1975.
11. *Petracca, Carmine, and James D. Lindberg,* "Installation and Operation of an Atmospheric Particulate Collector," ECOM-5575, September 1975.
12. Avara, Elton P., and George Alexander, "Empirical Investigation of Three Iterative Methods for Inverting the Radiative Transfer Equation," ECOM-5576, October 1975.
13. Alexander, George D., "A Digital Data Acquisition Interface for the SMS Direct Readout Ground Station - Concept and Preliminary Design," ECOM-5577, October 1975.
14. Cantor, Israel, "Enhancement of Point Source Thermal Radiation Under Clouds in a Nonattenuating Medium," ECOM-5578, October 1975.
15. Norton, Colburn, and Glenn Hoidale, "The Diurnal Variation of Mixing Height by Month over White Sands Missile Range, N.M," ECOM-5579, November 1975.
16. Avara, Elton P., "On the Spectrum Analysis of Binary Data," ECOM-5580, November 1975.
17. Taylor, Fredrick J., Thomas H. Pries, and Chao-Huan Huang, "Optimal Wind Velocity Estimation," ECOM-5581, December 1975.
18. Avara, Elton P., "Some Effects of Autocorrelated and Cross-Correlated Noise on the Analysis of Variance," ECOM-5582, December 1975.
19. Gillespie, Patti S., R.L. Armstrong, and Kenneth O. White, "The Spectral Characteristics and Atmospheric CO2 Absorption of the Ho:YLF Laser at 2.05μm," ECOM-5583, December 1975.
20. Novlan, David J. "An Empirical Method of Forecasting Thunderstorms for the White Sands Missile Range," ECOM-5584, February 1976.
21. Avara, Elton P., "Randomization Effects in Hypothesis Testing with Autocorrelated Noise," ECOM-5585, February 1976.
22. Watkins, Wendell R., "Improvements in Long Path Absorption Cell Measurement," ECOM-5586, March 1976.
23. Thomas, Joe, George D. Alexander, and Marvin Dubbin, "SATTEL - An Army Dedicated Meteorological Telemetry System," ECOM-5587, March 1976.
24. Kennedy, Bruce W., and Delbert Bynum, "Army User Test Program for the RDT&E-XM-75 Meteorological Rocket," ECOM-5588, April 1976.

25. Barnett, Kenneth M., "A Description of the Artillery Meteorological Observations at White Sands Missile Range, October 1974 – December 1974 (PASS)" Prototype Artillery Meteorological Support Study, ECOM-5589, April 1976.
26. Miller, Walter B., "Preliminary Analysis of Project Sigma Error, Project PASS," ECOM-5590, April 1976.
27. Avara, Elton P., "Error Analysis of Minimum Information and Smith's Direct Methods for Inverting the Radiative Transfer Equation," ECOM-5591, April 1976.
28. Yee, Youn, P., James D. Horn, and George Alexander, "Synoptic Thermal Wind Calculations from Radiosonde Observations Over the Southwestern United States," ECOM-5592, May 1976.
29. Duncan, Louis D., and Mary Ann Seagraves, "Applications of Empirical Corrections to NOAA-4 VTPR Observations," ECOM-5593, May 1976.
30. Miers, Bruce T., and Steve Weaver, "Applications of Meteorological Satellite Data to Weather Sensitive Army Operations," ECOM-5594, May 1976.
31. Sharenow, Moses, "Redesign and Improvement of Balloon ML-566," ECOM-5595, June, 1976.
32. Hansen, Frank V., "The Depth of the Surface Boundary Layer," ECOM-5596, June 1976.
33. Pinnick, R.G., and E.B. Stenmark, "Response Calculations for a Commercial Light-Scattering Aerosol Counter," ECOM-5597, July 1976.
34. Mason, J., and G.B. Hoidale, "Visibility as an Estimator of Infrared Transmittance," ECOM-5598, July 1976.
35. Bruce, Rufus E., Louis D. Duncan, and Joseph H. Pierlussi, "Experimental Study of the Relationship Between Radiosonde Temperatures and Radiometric Area Temperatures," ECOM-5599, August 1976.
36. Duncan, Louis D., "Stratospheric Wind Shear Computed from Satellite Thermal Sounder Measurements," ECOM-5800, September 1976.
37. Taylor, F., P. Mohan, P. Joseph and T. Pries, "An All Digital Automated Wind Measurement System," ECOM-5801, September 1976.
38. Bruce, Charles, "Development of Spectrophones for CW and Pulsed Radiation Sources," ECOM-5802, September 1976.
39. Duncan, Louis D., and Mary Ann Seagraves, "Another Method for Estimating Clear Column Radiances," ECOM-5803, October 1976.
40. Blanco, Abel J., and Larry E. Taylor, "Artillery Meteorological Analysis of Project Pass," ECOM-5804, October 1976.
41. Miller, Walter, and Bernard Engebos, "A Mathematical Structure for Refinement of Sound Ranging Estimates," ECOM-5805, November, 1976.
42. Gillespie, James B., and James D. Landberg, "A Method to Obtain Diffuse Reflectance Measurements from 1.0 to 3.0 μm Using a Cary 171 Spectrophotometer," ECOM-5806, November 1976.
43. Rubio, Roberto, and Robert O. Olsen, "A Study of the Effects of Temperature Variations on Radio Wave Absorption," ECOM-5807, November 1976.
44. Ballard, Harold N., "Temperature Measurements in the Stratosphere from Balloon-Borne Instrument Platforms, 1968-1975," ECOM-5808, December 1976.
45. Monahan, H.H., "An Approach to the Short Range Prediction of Early Morning Radiation Fog," ECOM-5809, January 1977.
46. Engebos, Bernard Francis, "Introduction to Multiple State Multiple Action Decision Theory and Its Relation to Mixing Structures," ECOM 5810, January 1977.
47. Low, Richard D.H., "Effects of Cloud Particles on Remote Sensing from Space in the 10-Micrometer Infrared Region," ECOM-5811, January 1977.
48. Bonner, Robert S., and R. Newton, "Application of the AN GVS-5 Laser Rangefinder to Cloud Base Height Measurements," ECOM-5812, February 1977.
49. Rubio, Roberto, "Lidar Detection of Subvisible Reentry Vehicle Erosive Atmospheric Material," ECOM-5813, March 1977.
50. Low, Richard D.H., and J.D. Horn, "Mesoscale Determination of Cloud Top Height Problems and Solutions," ECOM-5814, March 1977.

51. Duncan, Louis D., and Mary Ann Seagraves, "Evaluation of the NOAA-4 VTPR Thermal Winds for Nuclear Fallout Predictions," ECOM-5815, March 1977.
52. Randhawa, Jagir S., M. Izquierdo, Carlos McDonald and Zvi Salpeter, "Stratospheric Ozone Density as Measured by a Chemiluminescent Sensor During the Stratcom VI-A Flight," ECOM-5816, April 1977.
53. Rubio, Roberto, and Mike Izquierdo, "Measurements of Net Atmospheric Irradiance in the 0.7- to 2.8-Micrometer Infrared Region," ECOM-5817, May 1977.
54. Ballard, Harold N., Jose M. Serna, and Frank P. Hudson Consultant for Chemical Kinetics, "Calculation of Selected Atmospheric Composition Parameters for the Mid-Latitude, September Stratosphere," ECOM-5818, May 1977.
55. Mitchell, J.D., R.S. Sagar, and R.O. Olsen, "Positive Ions in the Middle Atmosphere During Sunrise Conditions," ECOM-5819, May 1977.
56. White, Kenneth O., Wendell R. Watkins, Stuart A. Schleusener, and Ronald L. Johnson, "Solid-State Laser Wavelength Identification Using a Reference Absorber," ECOM-5820, June 1977.
57. Watkins, Wendell R., and Richard G. Dixon, "Automation of Long-Path Absorption Cell Measurements," ECOM-5821, June 1977.
58. Taylor, S.E., J.M. Davis, and J.B. Mason, "Analysis of Observed Soil Skin Moisture Effects on Reflectance," ECOM-5822, June 1977.
59. Duncan, Louis D. and Mary Ann Seagraves, "Fallout Predictions Computed from Satellite Derived Winds," ECOM-5823, June 1977.
60. Snider, D.E., D.G. Murcray, F.H. Murcray, and W.J. Williams, "Investigation of High-Altitude Enhanced Infrared Background Emissions" (U), SECRET, ECOM-5824, June 1977.
61. Dubbin, Marvin H. and Dennis Hall, "Synchronous Meteorological Satellite Direct Readout Ground System Digital Video Electronics," ECOM-5825, June 1977.
62. Miller, W., and B. Engebos, "A Preliminary Analysis of Two Sound Ranging Algorithms," ECOM-5826, July 1977.
63. Kennedy, Bruce W., and James K. Luers, "Ballistic Sphere Techniques for Measuring Atomspheric Parameters," ECOM-5827, July 1977
64. Duncan, Louis D., "Zenith Angle Variation of Satellite Thermal Sounder Measurements," ECOM-5828, August 1977.
65. Hansen, Frank V., "The Critical Richardson Number," ECOM-5829, September 1977.
66. Ballard, Harold N., and Frank P. Hudson (Compilers), "Stratospheric Composition Balloon-Borne Experiment," ECOM-5830, October 1977.
67. Barr, William C., and Arnold C. Peterson, "Wind Measuring Accuracy Test of Meteorological Systems," ECOM-5831, November 1977.
68. Ethridge, G.A. and F.V. Hansen, "Atmospheric Diffusion: Similarity Theory and Empirical Derivations for Use in Boundary Layer Diffusion Problems," ECOM-5832, November 1977.
69. Low, Richard D.H., "The Internal Cloud Radiation Field and a Technique for Determining Cloud Blackness," ECOM 5833, December 1977.
70. Watkins, Wendell R., Kenneth O. White, Charles W. Bruce, Donald L. Walters, and James D. Lindberg, "Measurements Required for Prediction of High Energy Laser Transmission," ECOM-5834, December 1977.
71. Rubio, Robert, "Investigation of Abrupt Decreases in Atmospherically Backscattered Laser Energy," ECOM-5835, December 1977.
72. Monahan, H.H. and R.M. Cionco, "An Interpretative Review of Existing Capabilities for Measuring and Forecasting Selected Weather Variables (Emphasizing Remote Means)," ASL-TR-0001, January 1978.
73. Heaps, Melvin G., "The 1979 Solar Eclipse and Validation of D-Region Models," ASL-TR-0002, March 1978.

74. Jennings, S.G., and J.B. Gillespie, "M.I.E. Theory Sensitivity Studies - The Effects of Aerosol Complex Refractive Index and Size Distribution Variations on Extinction and Absorption Coefficients Part II: Analysis of the Computational Results," ASL-TR-0003, March 1978.
75. White, Kenneth O. et al, "Water Vapor Continuum Absorption in the 3.5μm to 4.0μm Region," ASL-TR-0004, March 1978.
76. Olsen, Robert O., and Bruce W. Kennedy, "ABRES Pretest Atmospheric Measurements," ASL-TR-0005, April 1978.
77. Ballard, Harold N., Jose M. Serna, and Frank P. Hudson, "Calculation of Atmospheric Composition in the High Latitude September Stratosphere," ASL-TR-0006, May 1978.
78. Watkins, Wendell R. et al, "Water Vapor Absorption Coefficients at HF Laser Wavelengths," ASL-TR-0007, May 1978.
79. Hansen, Frank V., "The Growth and Prediction of Nocturnal Inversions," ASL-TR-0008, May 1978.
80. Samuel, Christine, Charles Bruce, and Ralph Brewer, "Spectrophone Analysis of Gas Samples Obtained at Field Site," ASL-TR-0009, June 1978.
81. Pinnick, R.G. et al., "Vertical Structure in Atmospheric Fog and Haze and its Effects on IR Extinction," ASL-TR-0010, July 1978.
82. Low, Richard D.H., Louis D. Duncan, and Richard B. Gomez, "The Microphysical Basis of Fog Optical Characterization," ASL-TR-0011, August 1978.
83. Heaps, Melvin G., "The Effect of a Solar Proton Event on the Minor Neutral Constituents of the Summer Polar Mesosphere," ASL-TR-0012, August 1978.
84. Mason, James B., "Light Attenuation in Falling Snow," ASL-TR-0013, August 1978.
85. Blanco, Abel J., "Long-Range Artillery Sound Ranging: "PASS" Meteorological Application," ASL-TR-0014, September 1978.
86. Heaps, M.G., and F.E. Niles, "Modeling the Ion Chemistry of the *D-Region*: A case Study Based Upon the 1966 Total Solar Eclipse," ASL-TR-0015, September 1978.
87. Jennings, S.G., and R.G. Pinnick, "Effects of Particulate Complex Refractive Index and Particle Size Distribution Variations on Atmospheric Extinction and Absorption for Visible Through Middle-Infrared Wavelengths," ASL-TR-0016, September 1978.
88. Watkins, Wendell R., Kenneth O. White, Lanny R. Bower, and Brian Z. Sojka, "Pressure Dependence of the Water Vapor Continuum Absorption in the 3.5- to 4.0-Micrometer Region," ASL-TR-0017, September 1978.
89. Miller, W.B., and B.F. Engebos, "Behavior of Four Sound Ranging Techniques in an Idealized Physical Enviroment," ASL-TR-0018, September 1978.
90. Gomez, Richard G., "Effectiveness Studies of the CBU-88 B Bomb, Cluster, Smoke Weapon" (U), CONFIDENTIAL ASL-TR-0019, September 1978.
91. Miller, August, Richard C. Shirkey, and Mary Ann Seagraves, "Calculation of Thermal Emission from Aerosols Using the Doubling Technique," ASL-TR-0020, November, 1978.
92. Lindberg, James D. et al., "Measured Effects of Battlefield Dust and Smoke on Visible, Infrared, and Millimeter Wavelengths Propagation: A Preliminary Report on Dusty Infrared Test-1 (DIRT-1)," ASL-TR-0021, January 1979.
93. Kennedy, Bruce W., Arthur Kinghorn, and B.R. Hixon, "Engineering Flight Tests of Range Meteorological Sounding System Radiosonde," ASL-TR-0022, February 1979.
94. Rubio, Roberto, and Don Hoock, "Microwave Effective Earth Radius Factor Variability at Wiesbaden and Balboa," ASL-TR-0023, February 1979.
95. Low, Richard D.H., "A Theoretical Investigation of Cloud/Fog Optical Properties and Their Spectral Correlations," ASL-TR-0024, February 1979.

96. Pinnick, R.G., and H.J. Auvermann, "Response Characteristics of Knollenberg Light-Scattering Aerosol Counters," ASL-TR-0025, February 1979.
97. Heaps, Melvin G., Robert O. Olsen, and Warren W. Berning, "Solar Eclipse 1979, Atmospheric Sciences Laboratory Program Overview," ASL-TR-0026 February 1979.
98. Blanco, Abel J., "Long-Range Artillery Sound Ranging: 'PASS' GR-8 Sound Ranging Data," ASL-TR-0027, March 1979.
99. Kennedy, Bruce W., and Jose M. Serna, "Meteorological Rocket Network System Reliability," ASL-TR-0028, March 1979.
100. Swingle, Donald M., "Effects of Arrival Time Errors in Weighted Range Equation Solutions for Linear Base Sound Ranging," ASL-TR-0029, April 1979.
101. Umstead, Robert K., Ricardo Pena, and Frank V. Hansen, "KWIK: An Algorithm for Calculating Munition Expenditures for Smoke Screening/Obscuration in Tactical Situations," ASL-TR-0030, April 1979.
102. D'Arcy, Edward M., "Accuracy Validation of the Modified Nike Hercules Radar," ASL-TR-0031, May 1979.
103. Rodriguez, Ruben, "Evaluation of the Passive Remote Crosswind Sensor," ASL-TR-0032, May 1979.
104. Barber, T.L., and R. Rodgriquez, "Transit Time Lidar Measurement of Near-Surface Winds in the Atmosphere," ASL-TR-0033, May 1979.
105. Low, Richard D.H., Louis D. Duncan, and Y.Y. Roger R. Hsiao, "Microphysical and Optical Properties of California Coastal Fogs at Fort Ord," ASL-TR-0034, June 1979.
106. Rodriguez, Ruben, and William J. Vechione, "Evaluation of the Saturation Resistant Crosswind Sensor," ASL-TR-0035, July 1979.
107. Ohmstede, William D., "The Dynamics of Material Layers," ASL-TR-0036, July 1979.
108. Pinnick, R.G., S.G. Jennings, Petr Chylek, and H.J. Auvermann "Relationships between IR Extinction, Absorption, and Liquid Water Content of Fogs," ASL-TR-0037, August 1979.
109. Rodriguez, Ruben, and William J. Vechione, "Performance Evaluation of the Optical Crosswind Profiler," ASL-TR-0038, August 1979.
110. Miers, Bruce T., "Precipitation Estimation Using Satellite Data" ASL-TR-0039, September 1979.
111. Dickson, David H., and Charles M. Sonnenschein, "Helicopter Remote Wind Sensor System Description," ASL-TR-0040, September 1979.
112. Heaps, Melvin, G., and Joseph M. Heimerl, "Validation of the Dairchem Code, I: Quiet Midlatitude Conditions," ASL-TR-0041, September 1979.
113. Bonner, Robert S., and William J. Lentz, "The Visioceilometer: A Portable Cloud Height and Visibility Indicator," ASL-TR-0042, October 1979.
114. Cohn, Stephen L., "The Role of Atmospheric Sulfates in Battlefield Obscurations," ASL-TR-0043, October 1979.
115. Fawbush, E.J. et al, "Characterization of Atmospheric Conditions at the High Energy Laser System Test Facility (HELSTF), White Sands Missile Range, New Mexico, Part I, 24 March to 8 April 1977," ASL-TR-0044, November 1979
116. Barber, Ted L., "Short-Time Mass Variation in Natural Atmospheric Dust," ASL-TR-0045, November 1979
117. Low, Richard D.H., "Fog Evolution in the Visible and Infrared Spectral Regions and its Meaning in Optical Modeling," ASL-TR-0046, December 1979
118. Duncan, Louis D. et al, "The Electro-Optical Systems Atmospheric Effects Library, Volume I: Technical Documentation, ASL-TR-0047, December 1979.
119. Shirkey, R. C. et al, "Interim E-O SAEL, Volume II, Users Manual," ASL-TR-0048, December 1979.
120. Kobayashi, H.K., "Atmospheric Effects on Millimeter Radio Waves," ASL-TR-0049, January 1980.
121. Seagraves, Mary Ann and Duncan, Louis D., "An Analysis of Transmittances Measured Through Battlefield Dust Clouds," ASL-TR-0050, February, 1980.

122. Dickson, David H., and Jon E. Ottesen, "Helicopter Remote Wind Sensor Flight Test," ASL-TR-0051, February 1980.
123. Pinnick, R. G., and S. G. Jennings, "Relationships Between Radiative Properties and Mass Content of Phosphoric Acid, HC, Petroleum Oil, and Sulfuric Acid Military Smokes," ASL-TR-0052, April 1980.
124. Hinds, B. D., and J. B. Gillespie, "Optical Characterization of Atmospheric Particulates on San Nicolas Island, California," ASL-TR-0053, April 1980.
125. Miers, Bruce T., "Precipitation Estimation for Military Hydrology," ASL-TR-0054, April 1980.
126. Stenmark, Ernest B., "Objective Quality Control of Artillery Computer Meteorological Messages," ASL-TR-0055, April 1980.
127. Duncan, Louis D., and Richard D. H. Low, "Bimodal Size Distribution Models for Fogs at Meppen, Germany," ASL-TR-0056, April 1980.
128. Olsen, Robert O., and Jagir S. Randhawa, "The Influence of Atmospheric Dynamics on Ozone and Temperature Structure," ASL-TR-0057, May 1980.
129. Kennedy, Bruce W., et al, "Dusty Infrared Test-II (DIRT-II) Program," ASL-TR-0058, May 1980.
130. Heaps, Melvin G., Roberts O. Olsen, Warren Berning, John Cross, and Arthur Gilcrease, "1979 Solar Eclipse, Part I - Atmospheric Sciences Laboratory Field Program Summary," ASL-TR-0059, May 1980.
131. Miller, Walter B., "User's Guide for Passive Target Acquisition Program Two (PTAP-2)," ASL-TR-0060, June 1980.
132. Holt, E. H., H. H. Monahan, and E. J. Fawbush, "Atmospheric Data Requirements for Battlefield Obscuration Applications," ASL-TR-0061, June 1980.
133. Shirkey, Richard C., August Miller, George H. Goedecke, and Yugal Behl, "Single Scattering Code AGAUSX: Theory, Applications, Comparisons, and Listing," ASL-TR-0062, July 1980.
134. Sojka, Brain Z., and Kenneth O. White, "Evaluation of Specialized Photoacoustic Absorption Chambers for Near-millimeter Wave (NMMW) Propagation Measurements," ASL-TR-0063, August 1980.
135. Bruce, Charles W., Young Paul Yee, and S. G. Jennings, "In Situ Measurement of the Ratio of Aerosol Absorption to Extinction Coefficient," ASL-TR-0064, August 1980.
136. Yee, Young Paul, Charles W. Bruce, and Ralph J. Brewer, "Gaseous Particulate Absorption Studies at WSMR using Laser Sourced Spectrophones," ASL-TR-0065, June 1980.
137. Lindberg, James D., Radon B. Loveland, Melvin Heaps, James B. Gillespie, and Andrew F. Lewis, "Battlefield Dust and Atmospheric Characterization Measurements During West German Summertime Conditions in Support of Grafenwohr Tests," ASL-TR-0066, September 1980.
138. Vechione, W. J., "Evaluation of the Environmental Instruments, Incorporated Series 200 Dual Component Wind Set," ASL-TR-0067, September 1980.

★ U.S. GOVERNMENT PRINTING OFFICE 1980 0 777 026 2